

Differential Expression and Function of Alternative Splicing Variants of Human Liver X Receptor α

Kaori Endo-Umeda, Shigeyuki Uno, Ko Fujimori, Yoshikazu Naito, Koichi Saito, Kenji Yamagishi, Yangsik Jeong, Hiroyuki Miyachi, Hiroaki Tokiwa, Sachiko Yamada, and Makoto Makishima

Division of Biochemistry, Department of Biomedical Sciences [K.E., S.U., S.Y., M.M.], Nihon University School of Medicine, 30-1 Oyaguchi-kamicho, Itabashi-ku, Tokyo 173-8610, Japan; Laboratory of Biodefense and Regulation [K.F.], Osaka University of Pharmaceutical Sciences, 4-20-1 Nasahara, Takatsuki, Osaka, Japan; Environmental Health Science Laboratory [Y.N., K.S.], Sumitomo Chemical Co., Ltd., 3-1-98 Kasugade-naka, Konohana-ku, Osaka, Japan; Research Information Center for Extremophile [K.Y.], and Department of Chemistry [H.T.], Faculty of Science, Rikkyo University, 3-34-1 Nishi-Ikebukuro, Toshima-ku, Tokyo, Japan; Department of Biochemistry, Institute of Lifestyle Medicine, and Nuclear Receptor Research Consortium [Y.J.], Yonsei University Wonju College of Medicine, 162 Ilsan-dong, Wonju-si, Gangwon-do, Republic of Korea; Graduate School of Medicine, Dentistry and Pharmaceutical Sciences [H.M.], Okayama University, 1-1-1 Tsushima-Naka, Kita-ku, Okayama 700-8530, Japan

Running title: Liver X receptor α ligand-binding domain variants

Address correspondence to: Makoto Makishima, Division of Biochemistry, Department of Biomedical Sciences, 30-1 Oyaguchi-kamicho, Itabashi-ku, Tokyo 173-8610, Japan.

E-mail address: makishima.makoto@nihon-u.ac.jp.

Number of text pages: 44

Number of figures: 10

Number of tables: 2

Number of references: 35

Number of words in Abstract: 249

Number of words in Introduction: 349

Number of words in Discussion: 810

Abbreviations: LXR, liver X receptor; LXRE, LXR-responsive element; RXR, retinoid X receptor; ABC, ATP-binding cassette; CYP7A, cholesterol 7 α -hydroxylase; SREBP-1c, sterol regulatory element-binding protein-1c; LBD, ligand-binding domain; FBS, fetal bovine serum; PCR, polymerase chain reaction; EMSA, electrophoretic mobility shift assay; DBD, DNA-binding domain; AF2 activation function 2; SMRT, silencing mediator of retinoic acid and thyroid hormone receptor; N-CoR, nuclear receptor

MOL #77206

co-repressor; SRC-1, steroid receptor coactivator 1; DRIP205, vitamin D
receptor-interacting protein 205; PPAR γ , peroxisome proliferator-activated receptor γ .

Abstract

The liver X receptor α (LXR α) is a nuclear receptor that is involved in regulation of lipid metabolism, cellular proliferation and apoptosis, and immunity. In this report, we characterize three human LXR α isoforms with variation in the ligand-binding domain (LBD). While examining the expression of LXR α 3, which lacks 60 amino acids within the LBD, we identified two novel transcripts, which encode LXR α -LBD variants (LXR α 4 and LXR α 5). LXR α 4 has an insertion of 64 amino acids in helix 4/5, and LXR α 5 lacks the C-terminal helices 7-12 due to a termination codon in an additional exon that encodes an intron in the LXR α 1 mRNA. LXR α 3, LXR α 4 and LXR α 5 were expressed at lower levels when compared with LXR α 1 in many human tissues and cell lines. We also observed weak expression of LXR α 3 and LXR α 4 in several tissues of mice. LXR ligand treatment induced differential regulation of LXR α isoform mRNA expression in a cell type-dependent manner. While LXR α 3 had no effect, LXR α 4 has weak transactivation, RXR heterodimerization, and coactivator recruitment activities. LXR α 5 interacted with a corepressor in a ligand-independent manner and inhibited LXR α 1 transactivation and target gene expression when overexpressed. Combination of LXR α 5 cotransfection and LXR α antagonist treatment produced additive effects on the inhibition of ligand-dependent LXR α 1 activation. We constructed structural models of the LXR α 4-LBD and its complexes with ligand, RXR-LBD and coactivator peptide. The models showed that the insertion in the LBD can be predicted to disrupt RXR

heterodimerization. Regulation of LXR α pre-mRNA splicing may be involved in the pathogenesis of LXR α -related diseases.

Introduction

Liver X receptor α (LXR α ; NR1H3) and LXR β (NR1H2) are transcription factors of the nuclear receptor superfamily (Makishima, 2005; Tontonoz and Mangelsdorf, 2003). Whereas LXR β is ubiquitously expressed, LXR α is localized to the liver, adipose tissue, small intestine, and macrophages. Both receptors are activated by oxysterols and have been linked to pathways involved in fatty acid and cholesterol homeostasis. LXRs bind preferentially to LXR-responsive elements (LXREs) that consist of a two hexanucleotide (AGGTCA or a related sequence) direct repeat motif separated by four nucleotides (direct repeat 4) as a heterodimer with retinoid X receptor (RXR; NR2B). LXRs regulate intestinal absorption and biliary excretion of cholesterol by inducing the expression of target genes such as the ATP-binding cassette (ABC) transporters ABCA1, ABCG5, and ABCG8 (Repa and Mangelsdorf, 2002; Tontonoz and Mangelsdorf, 2003). LXR α stimulates the conversion of cholesterol to bile acids by cholesterol 7 α -hydroxylase (CYP7A) in rodents. LXRs stimulate reverse cholesterol transport from peripheral tissues and exhibit antiatherogenic activity. LXR activation also stimulates lipogenesis in the liver by inducing lipogenic genes, including sterol regulatory element-binding protein-1c (SREBP-1c), fatty acid synthase and stearoyl-coenzyme A desaturase-1 (Schultz et al., 2000). Studies using LXR-null mice and synthetic LXR ligands have also demonstrated that LXRs are involved in the regulation of cellular proliferation and apoptosis (Blaschke et al., 2004; Joseph et al., 2004; Uno et al., 2009; Valledor et al., 2004).

Three human LXR α isoforms (α 1, α 2, and α 3) have been identified that are derived from a single gene as a result of alternate promoter usage and alternative splicing of pre-mRNA (Chen et al., 2005). LXR α 1 is the originally identified isoform (Willy et al., 1995), LXR α 2 lacks the N-terminal 45 amino acids of LXR α 1, and LXR α 3 lacks 50 amino acids in the ligand-binding domain (LBD) (Chen et al., 2005). Like different isoforms of other nuclear receptors, LXR α isoforms have distinct expression patterns and altered transcriptional activity, suggesting that the expression of the isoforms modulates LXR signaling. In this study, we isolated and identified two novel LXR α isoforms, LXR α 4 and LXR α 5, and investigated the roles of LXR α isoforms with functional assays and molecular modeling studies.

Materials and Methods

Chemical Compounds. T0901317

[*N*-(2,2,2-trifluoro-ethyl)-*N*-[4-(2,2,2-trifluoro-1-hydroxy-1-trifluoromethyl-ethyl)-phenyl]-benzenesulfonamide]] was purchased from Cayman Chemical Company (Ann Arbor, MI), 24(*S*),25-epoxycholesterol was from Enzo Life Science (Farmingdale, NY), 22(*R*)-hydroxycholesterol and 22(*S*)-hydroxycholesterol were from Steraroids (Newport, RI), and arachidonic acid and linolenic acid were from Sigma-Aldrich (St. Louis, MO).

GW3965

[3-[3-[*N*-(2-chloro-3-trifluoromethylbenzyl)-(2,2-diphenylethyl)amino]propyloxy]phenylacetic acid hydrochloride] was synthesized as reported previously (Noguchi-Yachide et al., 2007).

Cell Culture. Human kidney HEK293 cells (RIKEN Cell Bank, Tsukuba, Japan) were cultured in Dulbecco's modified Eagle medium containing 5% fetal bovine serum (FBS), 100 unit/ml penicillin, and 100 µg/ml streptomycin at 37°C in a humidified atmosphere containing 5% CO₂. Human hepatocellular carcinoma HepG2 (RIKEN Cell Bank), colon carcinoma HCT116, SW480, teratocarcinoma NT2/D1 (American Type Culture Collection, Rockville, MD), and immortalized keratinocyte HaCaT cells (kindly provided by Dr. Tadashi Terui, Department of Dermatology, Nihon University School of Medicine) were cultured in Dulbecco's modified Eagle medium containing 10% FBS. Human colon carcinoma Caco-2, osteosarcoma MG63, neuroblastoma SK-N-SH cells

(RIKEN Cell Bank) were maintained in MEM containing 10% FBS, and myeloid leukemia U937, HL60, THP-1 (RIKEN Cell Bank), and breast carcinoma MCF-7 cells (American Type Culture Collection) were in RPMI 1640 medium containing 10% FBS.

Animals. C57BL/6J mice were obtained from Charles River Laboratories Japan (Yokohama, Japan) and $Lxr\alpha^{-/-}/Lxr\beta^{-/-}$ mice were provided by Dr. Mangelsdorf, University of Texas Southwestern Medical Center at Dallas, TX (Repa et al., 2000). Mice were maintained under controlled temperature (23 ± 1 °C) and humidity (45-65%) with free access to water and chow (Lab. Animal Diet MF; Oriental Yeast, Tokyo, Japan). Tissue samples were collected from male mice between 8 and 9 weeks of age. The experimental protocol adhered to the Guidelines for Animal Experiments of the Nihon University School of Medicine and was approved by the Ethics Review Committee for Animal Experimentation of Nihon University School of Medicine.

Reverse Transcription and Real-time Quantitative Polymerase Chain Reaction.

Total RNAs from samples were prepared by the acid guanidine thiocyanate-phenol/chloroform method (Ishizawa et al., 2008). cDNAs were synthesized using the ImProm-II Reverse Transcription system (Promega Corporation, Madison, WI). cDNA panels of several human tissues were purchased from Takara Bio Inc. (Otsu, Japan). Real-time polymerase chain reaction (PCR) was performed on the ABI PRISM 7000 Sequence Detection System (Applied Biosystems, Foster City, CA) using Power SYBR Green PCR Master Mix (Applied Biosystems). Primer sequences are listed in

Tables 1 and 2. The mRNA values were normalized to the expression level of glyceraldehyde-3-phosphate dehydrogenase mRNA.

RNA Interference. Small interfering RNAs (siRNAs) directed against LXR α (LXR α -siRNA-1; Dharmacon M-003413-01-0005) and control siRNA were purchased from Thermo Fisher Scientific (Waltham, MA). siRNAs against LXR α (LXR α -siRNA-2; 5'-AGAAAC UGA AGC GGC AAG A-3') and LXR α/β (LXR α/β -siRNA; 5'-CAU CAA CCC CAU CUU CGA G-3') were designed by the Jeong laboratory. siRNA oligonucleotides were transfected into HaCaT cells and HepG2 cells using DharmaFECT1 Reagent (Thermo Fisher Scientific) and Trans IT-TKO Reagent (Mirus Bio, Madison, WI), respectively, according to the manufacturer's instructions.

Western Blotting Analysis. For endogenous LXR proteins, nuclear extracts were prepared as described previously (Inaba et al., 2007). The proteins were separated by SDS-PAGE and were transferred to a nitrocellulose membrane, probed with anti-LXR α antibody (Perseus Proteomics Inc., Tokyo, Japan), and visualized by enhanced chemiluminescence. For exogenous FLAG-tagged LXR proteins, whole cell lysates from transfected HEK293 cells were subjected to Western blotting with anti-FLAG antibody (Sigma-Aldrich), visualized by an alkaline phosphatase conjugate substrate system.

Plasmids. Fragments of the original isoform LXR α 1 (GenBank accession no. NM_005693) (Willy et al., 1995), the previously reported isoform LXR α 3 (GenBank accession no. NM_001130101) (Chen et al., 2005), and newly identified isoforms

(LXR α 4 and LXR α 5) (Fig. 1) were inserted into pFLAG-CMV2 (Sigma-Aldrich) to make pFLAG-CMV2-LXR α 1, pFLAG-CMV2-LXR α 3, pFLAG-CMV2-LXR α 4, and pFLAG-CMV2-LXR α 5, respectively. The VP16 fragment from pCMX-VP16 was inserted into pFLAG-CMV2-LXR α plasmids to make pFLAG-CMV2-VP16-LXR α isoforms (Kaneko et al., 2003). The LBDs from each LXR α isoform were inserted to pCMX-GAL4 vectors to make pCMX-GAL4-LXR α isoforms. The expression vectors pCMX- β -catenin-MT, pCMX-GAL4, pCMX-GAL4-RXR α , pCMX-VP16-RXR α , pCMX-GAL4-SRC1, pCMX-GAL4-DRIP205, pCMX-GAL4-SMRT, pCMX-GAL4-N-CoR, the luciferase reporters (rCyp7a-DR4)x3-tk-LUC, TOP-GLOW, and MH100(UAS)x4-tk-LUC reporters were used as reported previously (Inaba et al., 2007; Kaneko et al., 2003; Uno et al., 2009).

Transfection Assay. Transfections in HEK293 cells were performed by the calcium phosphate coprecipitation method (Kaneko et al., 2003; Uno et al., 2009). Eight hours after transfection, compounds were added. Cells were harvested after 16-18 hours, and were assayed for luciferase and β -galactosidase activities using a luminometer and a microplate reader (Molecular Devices Sunnyvale, CA). For most experiments, transfection experiments used 50 ng of reporter plasmid, 10 ng of pCMX- β -galactosidase, and 15 ng of each expression plasmid in each well of a 96-well plate. Luciferase data were normalized to the internal β -galactosidase control. SW480 cells were transfected 2.5 μ g of expression plasmid by FuGene HD (Roche Applied Science, Indianapolis, IN).

Electrophoretic Mobility Shift Assays. Electrophoretic mobility shift assays (EMSAs) were performed as reported previously (Chen et al., 2005; Yoshikawa et al., 2001). Briefly, receptor proteins were in vitro translated with a TNT Quick Coupled Transcription/Translation System (Promega Corporation). Double stranded oligonucleotides for LXREs were 5'-CAG TGA CCG CCA GTA ACC CCA GC-3' (LXREa) and 5'-GGA CGC CCG CTA GTA ACC CCG GC-3' (LXREb) from the mouse SREBP-1c promoter (Yoshikawa et al., 2001), 5'-GCT TTG GTC ACT CAA GTT CAA GTT A-3' from the rat CYP7A promoter (Lu et al., 2000), and 5'- GAT CAC GAT GAC CGG TAG TAA CCC CGC C-3' from the rat fatty acid synthase (Chen et al., 2005). Binding reactions were performed in a buffer containing 10 mM Tris-HCl (pH 7.6), 50 mM KCl, 0.05 mM EDTA, 2.5 mM MgCl₂, 8.5% glycerol, 1 mM dithiothreitol, 0.5 µg/ml poly(dI-dC), 0.1% Triton-X100, and nonfat milk (Yoshikawa et al., 2001). Unlabeled probes and anti-LXR α antibody (Perseus Proteomics Inc.) were used for competition experiments and supershift experiments, respectively. Samples were separated on 5% polyacrylamide gels, visualized with autoradiography.

Molecular Modeling. The structure of the LXR α 4-LBD was manipulated using Sybyl 7.3 (Tripos, St. Louis, MO). We also used Swiss-Prot ExPASy proteomics tools for homology modeling of LXR α 4-LBD and alignment of LXR α isoforms. Energy minimization of the constructed models was performed on the Tripos force field. The atomic coordinates of the crystal structures of human LXR β -LBD complexes were

MOL #77206

retrieved from Protein Data Bank (code 1p8d) (Williams et al., 2003).

Results

Identification of Novel LXR α -LBD Variants. While examining the expression of the LXR α -LBD isoform reported in GenBank (accession number NM_001130101), as LXR α 3 by Chen et al. (Chen et al., 2005), by PCR on a human tissue cDNA panel, we identified two novel transcripts, which we will refer to as LXR α 4 and LXR α 5. While the LXR α 3 mRNA is generated by the removal of exon 6 through alternative splicing (Chen et al., 2005), the LXR α 4 mRNA includes 192 nucleotides from an intron between exon 6 and exon 7 of LXR α 1 (GenBank accession number NM_005693) (Willy et al., 1995) (Fig. 1A and B). LXR α 1, LXR α 3 and LXR α 4 proteins have 447, 387 and 551 amino acids, respectively (Fig. 1C). The LXR α 5 mRNA is transcribed by alternative splicing that generates an additional exon between exon 7 and exon 8. Since a stop codon exists in this exon, LXR α 5 protein truncates the C-terminal helices 7-12 and has 356 amino acids.

We examined mRNA expression of LXR α isoforms by real-time quantitative reverse transcription-PCR with specific primers for each isoform (Table 1). In normal human tissues, LXR α 1 was highly expressed in liver, spleen, testis, pancreas, and thymus (Fig. 2A). LXR α 3, LXR α 4 and LXR α 5 were expressed weakly in the liver, spleen, ovary, small intestine and colon. We next examined the expression LXR α isoforms in human hepatocyte-derived HepG2, intestinal mucosa-derived HCT116, SW480, Caco-2, myeloid-derived U937, HL60, THP-1, kidney epithelium-derived HEK293, mammary epithelium-derived MCF-7, osteoblast-derived MG63, neuron-derived NT2/D1,

SK-N-SH, and keratinocyte-derived HaCaT cells. LXR α 1 was the predominant isoform in the all examined cells (Fig. 2B). LXR α 3 was expressed with the exception of MG63 and SK-N-SH cells. Interestingly, LXR α 4 was more abundant than LXR α 3 in Caco-2 cells. LXR α 5 was detected only weakly in the cell lines.

We compared the mouse LXR α gene (GenBank accession number NC_000068.6) with the human LXR α gene (GenBank accession number NC_000011.9), and designed specific primers for mouse LXR α 3 and LXR α 4 (Table 2). We could not find a fragment corresponding to the additional exon for human LXR α 5 in the mouse LXR α gene. LXR α 3 and LXR α 4 were expressed weakly in the liver, kidney, intestine, spleen, heart and lung of mice (Fig. 2C). Expression of these isoforms was at background levels in LXR α /LXR β -double knockout mice. Interestingly, LXR α 4 was more abundant than LXR α 3 in the mice tissues.

To examine LXR α isoform proteins, we transfected HaCaT cells with control or three different siRNAs against LXR α and determined protein accumulation of LXR α isoforms. Transfection of siLXR α -1, siLXR α -2 and, to a lesser extent, siLXR α / β decreased LXR α 1 protein levels (Fig. 3A). We observed weak expression of LXR α 3 and LXR α 4 proteins. LXR α 3 protein decreased in cells treated with siLXR α -1 but not siLXR α -2 (Fig. 3A). While siLXR α -1 targets a mixture of sequences in exon 5, exon 6 and exon 8, siLXR α -2 is against sequences in exon 6, a region lost in LXR α 3 (Fig. 1C). Treatment with siLXR α -2 and siLXR α / β reduced LXR α 4 protein levels (Fig. 3). We

could not detect LXR α 5 protein in HaCaT cells. We also transfected HepG2 cells with siRNAs against LXR α . Similar to experiments in HaCaT cells, LXR α 1 and LXR α 4 protein levels decreased in HepG2 cells treated with siLXR α -1, siLXR α -2 and siLXR α / β (Fig. 3B). Treatment with siLXR α -1 and siLXR α / β also reduced LXR α 3 protein levels in HepG2 cells. These findings indicate that LXR α 3 and LXR α 4 proteins are present in cells, although at lower levels when compared with LXR α 1.

The promoter of the human LXR α gene contains LXREs and its expression is induced by LXR ligand treatment in macrophages, constituting a mechanism of positive autoregulation (Laffitte et al., 2001; Li et al., 2002). We examined the effect of a synthetic LXR ligand, T0901317, on the mRNA expression of LXR α isoforms. T0901317 increased the expression of LXR α 1 in HepG2, SW480, and THP-1 cells, but not in MCF-7 cells (Fig. 4). The expression of LXR α 4 and LXR α 5 was also induced by T0901317 in HepG2, SW480, and THP-1 cells. T0901317 increased the expression of LXR α 3 in SW480 cells but had no effect in HepG2 and THP-1 cells. Interestingly, LXR α 3 expression was decreased by T0901317 in MCF-7 cells. Thus, the expression of LXR α isoforms is regulated in a cell type-dependent manner.

Transactivation and Cofactor Interaction of LXR α Isoforms. To examine the transactivation activity of LXR α isoforms, we transiently transfected HEK293 cells with an LXR isoform expression vector and a luciferase reporter containing LXRE (Peet et al.,

1998). We observed exogenous LXR α isoform proteins in HEK293 cells with immunoblotting (Fig. 5A). T0901317 effectively induced LXR α 1 transactivation but had not effect on LXR α 3, as reported previously (Chen et al., 2005) (Fig. 5B). T0901317 at 10 nM induced maximal LXR α 1 transactivation, and it at 30 and 100 nM did not cause further induction. T0901317 activated LXR α 4 less effectively than LXR α 1 and LXR α 5 showed no transcriptional activity. We transfected cells with a VP16-LXR α chimeric receptor together with the LXR-responsive reporter. Due to ligand-independent activity, the luciferase activity of VP16 chimeric receptors assesses the interaction of the receptor and the binding element (Adachi et al., 2004). VP16-LXR α 1 induced luciferase activity in the absence of ligand (Fig. 5C), suggesting that VP16-LXR α 1 binds to an LXRE in a ligand-independent manner. Ligand addition further increased transactivation but only slightly. VP16-LXR α 3 was not effective either in the presence or absence of ligand. These findings suggest that VP16-LXR α 3 does not interact with an LXRE in cells. VP16-LXR α 4 induced luciferase activity in a ligand-dependent manner and VP16-LXR α 5 induced weak ligand-independent luciferase activity. We examined the subcellular localization of LXR α isoforms using green fluorescence protein-fused proteins and found that all isoforms were localized in the nucleus (data not shown). In addition to transactivation, LXR α exhibits ligand-dependent transrepression of several transcription factors, including β -catenin (Uno et al., 2009). T0901317 treatment inhibited β -catenin transactivation of T cell factor-mediated transcription in the presence

of LXR α 1, as reported previously (Uno et al., 2009). Ligand-dependent inhibition was not observed with cotransfection of LXR α 3, LXR α 4, or LXR α 5. Thus, LXR α 3, LXR α 4 and LXR α 5 are non-functional LXR α isoforms (Fig. 5D).

To examine the RXR heterodimerization of LXR α isoforms, we performed mammalian two-hybrid experiments using VP16-LXR α , GAL4-RXR α and a GAL4-responsive luciferase reporter. The full-length fragments of LXR α isoforms were fused to the VP16 transactivation domain and the RXR α -LBD was fused to GAL4 DNA-binding domain (DBD). VP16-LXR α 1 effectively interacted with GAL4-RXR α in a ligand-independent manner (Fig. 5E). T0901317 treatment did not cause further increase, suggesting maximal interaction of GAL4-RXR α and VP16-LXR α 1 in the absence of ligand. VP16-LXR α 4 made a weak interaction with GAL4-RXR α that was enhanced by T0901317 treatment. VP16-LXR α 3 and VP16-LXR α 5 did not interact with GAL4-RXR α in the presence or absence of ligand. We next examined the interaction of GAL4-LXR α and VP16-RXR α . The LBDs of LXR α isoforms were fused to GAL4-DBD and the full-length fragment of RXR α was fused to the VP16 domain. First, we examined the transactivation activity of GAL4-LXR α isoforms with cotransfection of a control VP16 vector, which does not interact with a GAL4 chimeric receptor. Among the GAL4-LXR α isoforms, only GAL4-LXR α 1 was activated by T0901317 (Fig. 5F). Next, we examined effect of cotransfection of GAL4-LXR α and VP16-RXR α . GAL4-LXR α 1 plus VP16-RXR α activated the luciferase reporter, indicating a

ligand-independent association of these receptors. Ligand addition further enhanced the interaction. While full-length fragments of receptors were fused to VP16 proteins, GAL4 chimeric receptors contain only LBDs of receptors. These structures may cause the difference in interaction between GAL4-RXR α /VP16-LXR α 1 and GAL4-LXR α 1/VP16-RXR α . Interactions were not observed between VP16-RXR α and GAL4-LXR α 3, GAL4-LXR α 4, or GAL4-LXR α 5 (Fig. 5F). Comparison of the VP16-RXR α /GAL4-LXR α 4 interaction with the GAL4-RXR α /VP16-LXR α 4 interaction suggests that unlike LXR α 1-LBD, LXR α 4-LBD cannot stably heterodimerize with RXR.

We examined direct binding of LXR α isoforms to LXREs by EMSAs. As reported previously (Yoshikawa et al., 2001), LXR α 1-RXR heterodimer bound to a LXRE from the SREBP-1c promoter (Fig. 6A). Incubation with anti-LXR α antibody induced a supershift of the LXR α 1-RXR DNA complex, and addition of unlabeled probes competed the binding of LXR α 1-RXR to labeled probes, confirming the specific binding of LXR α 1-RXR to the LXRE. Complex formation of LXR α 1-RXR-LXRE did not require ligand addition (Fig. 6B), consistent with a ligand-independent effect of VP16-LXR α 1 on an LXRE reporter in cells (Fig. 5B). In contrast, DNA complex was not observed for LXR α 3, LXR α 4 and LXR α 5 in combination with RXR, and T0901317 treatment was not effective (Fig. 6B).

We examined the effect of other LXR ligands on transactivation of LXR α isoforms.

A synthetic agonist, GW3965, and natural ligands, 24(*S*),25-epoxycholesterol and 22(*R*)-hydroxycholesterol, activated LXR α 4, but weaker than LXR α 1 (Fig. 7A). 22(*S*)-hydroxycholesterol, arachidonic acid and linolenic acid are LXR antagonists (Ou et al., 2001; Spencer et al., 2001). These LXR antagonists did not activate LXR α isoforms (Fig. 7A). 22(*S*)-Hydroxycholesterol and arachidonic acid inhibited transactivation of LXR α 1 and LXR α 4 induced by GW3965 and 24(*S*),25-epoxycholesterol (Fig. 7B).

Upon ligand binding, nuclear receptors undergo conformational changes in the cofactor binding site and the activation function 2 (AF2) helix, which result in the dissociation of corepressors, such as silencing mediator of retinoic acid and thyroid hormone receptor (SMRT) and nuclear receptor co-repressor (N-CoR), and recruitment of coactivators, such as steroid receptor coactivator 1 (SRC-1) and vitamin D receptor-interacting protein 205 (DRIP205) (Rosenfeld et al., 2006). We fused the receptor-interacting domains of transcriptional cofactors to the GAL4-DBD and examined the interaction of LXR α isoforms with cofactors in a mammalian two-hybrid assay. VP16-LXR α 1 associated with GAL4-SRC-1 and GAL4-DRIP205, and addition of ligand or cotransfection of RXR α enhanced these interactions (Fig. 8, A and B). VP16-LXR α 4 weakly interacted with GAL4-SRC-1 and GAL4-DRIP205 only when cells were cotransfected with RXR α . T0901317 had a small effect on these interactions. These coactivator recruitment may be related to weak transactivation of LXR α 4 (Fig. 5B). The LXR α 3 and LXR α 5 did not interact with the coactivators. VP16-LXR α 1 interacted

with GAL4-N-CoR, with VP16-LXR α 5 interacting weakly (Fig. 8C). T0901317 caused a modest dissociation of N-CoR from VP16-LXR α 1, but not from VP16-LXR α 5. VP16-LXR α 1 and VP16-LXR α 5 also interacted with GAL4-SMRT, but ligand addition did not affect these interactions (Fig. 8C). VP16-LXR α 3 and VP16-LXR α 4 did not associate with these corepressors. These experiments illustrate differential interactions of LXR α isoforms with cofactors.

We next examined the dominant negative effect of LXR α 3, LXR α 4 and LXR α 5 on LXR α 1 transactivation. When expressed together with LXR α 1 in transfection assays, LXR α 3 and LXR α 4 did not act as dominant-negative inhibitors and LXR α 5 inhibited LXR α 1 transactivation when expressed in excess (Fig. 9A). In EMSAs, we did not detect a complex of LXR α 5, RXR and LXREs from SREBP-1c, CYP7A or fatty acid synthase (Fig. 6C). Expression of LXR α 5 also suppressed ligand-dependent induction of LXR target genes in SW480 cells, SREBP-1c and ABCA1, while LXR α 1 enhanced expression of these genes (Fig. 9B). Combination of LXR α 5 cotransfection and LXR α antagonist treatment produced additive effects on the inhibition of LXR α 1 transactivation induced by LXR agonists (Fig. 9C).

Structural Model of LXR α 4. Of LXR α 3, LXR α 4 and LXR α 5, only LXR α 4 displays transactivation potential (Fig. 5). LXR α 4 has an identical amino acid sequence with LXR α 1 with the exception of a 64 amino acid residue insertion between Glu 296 and

Val 297 at the helix 4/5 of LXR α 1 (Fig. 1). In order to make homology models of the LXR α 4-LBD and its heterodimer with RXR-LBD, we first constructed a monomeric model of LXR α 4-LBD (amino acids 206-511), called model M1, using an automatic modeling system (Swiss Model version 8.05) on the Swiss-Prot ExPASy workspace and the coordinates of previously solved LXR β -LBD/24(S),25-epoxycholesterol structure (Protein Data Bank code 1p8d; 58.88% sequence identity with the LXR α 4-LBD) (Williams et al., 2003). We docked the LXR ligand T0901317 into M1 by extracting the crystal structure of the LXR α -LBD/RXR β -LBD/T0901317 complex (Protein Data bank code 1uhl) (Svensson et al., 2003) and optimized the liganded complex on the Tripos force field (1,000 steps of iteration) using Sybyl 7.3 (Tripos) to yield model M2 (Fig. 10A). The stereochemistry of M2 satisfied a Ramachandran plot analysis. In M2, the 64-amino acid insertion extrudes rearward from the side of helix 10/11 covering the dimer interface. Crystal structure analysis is needed to elucidate whether the inserted region is totally outside the canonical structure of the LBD. LXR α 4 forms an RXR heterodimer and induces an LXRE reporter activation although weakly, as shown in Fig. 5. The RXR heterodimerization interface utilizes helix 10/11, helix 9, loop 8-9 and helix 7 of the LBD (Gampe et al., 2000). The recently solved crystal structure of the peroxisome proliferator-activated receptor γ (PPAR γ)/RXR γ /DNA complex (Protein Data Bank code 3dzy) shows an additional dimer interface between PPAR γ -LBD (loop 1-3 and β -turn) and RXR γ -DBD (Chandra et al., 2008). The LXR α 4 insertion is suggested to prevent

heterodimerization at the interface with RXR. LXR α 4 may interact only at the β -turn side of the LBD with the DBD of the dimer partner as has been shown for PPAR γ in the RXR heterodimer crystal structure.

We next constructed a canonical heterodimer model of LXR α 4-LBD/RXR β -LBD, using the LXR α 1-LBD/RXR β -LBD structure (Protein Data bank code 1uhl) as a model. We overlaid LXR α 4-LBD in the liganded model M1 with LXR α 1-LBD in the crystal structure, replaced the LXR α 1-LBD with LXR α 4-LBD, and changed the dihedral angle (ψ and ϕ) at Ser 282 of LXR α 4-LBD to relieve hindrance between the insertion and RXR β . We optimized the complex of LXR α 4-LBD/RXR β -LBD accommodated with each ligand (3,000 steps of iterations) by fixing RXR β and the two ligands to generate heterodimer model M3 (Fig. 10B). With this optimization, the insertion changed conformation significantly and was packed in the cavity beneath the contact of helix 10/11 from each monomer. The main chain conformations of M3 were found to be in satisfactory region by Ramachandran plot analysis. The peptide fragment of SRC-1 was extracted from the LXR β -LBD/24(*S*),25-epoxycholesterol complex structure (Protein Data Bank code 1p8d) and was docked into M3 to create the model M4. In M4, important residues of the AF2 helix such as charge clamp residues, Lys 273 at helix 3 and Glu 441 at helix 12, occupy the correct positions and an LXXLL-containing coactivator peptide of SRC-1 is predicted to stably interact (Fig. 10C).

Discussion

We report two novel LXR α -LBD isoforms, LXR α 4 and LXR α 5. LXR α 4 maintains transactivation, DNA binding and RXR heterodimerization with weaker activity than LXR α 1. Structural modeling reveals that the 64-amino acid insertion at helix 4/5 disturbs RXR heterodimerization. LXR α agonist treatment increased the activity of LXR α 4, suggesting that ligand binding stabilizes the conformation of the LXR α 4/RXR heterodimer. Although ligand treatment recruited coactivators to LXR α 4, interaction of LXR α 4 with corepressors was not observed. The LXR α 4 insertion may disturb corepressor interaction. LXR α 5, a C-terminal truncated form, lacks helices 7-12, the AF2 domain and dimerization interface. As expected, LXR α 5 is deficient in transactivation and coactivator recruitment. Interestingly, LXR α 5 associated with corepressors. LXR α 5 cotransfection inhibited LXR α 1 activity in the overexpression experiment and ligand-dependent expression of endogenous LXR target genes (Fig. 9). LXR α 3 lacks the residues necessary for helices 3 and 4/5. LXR α 3 has an intact DBD and binds to an LXRE in combination with RXR in an in vitro EMSA (Chen et al., 2005). In contrast, we did not observe formation of a LXR α 3-RXR-LXRE complex in the absence or presence of LXR ligand (Fig. 6B). This discrepancy between our study and Chen et al. may be due to a difference in experimental conditions. Consistent with our EMSA results, LXR α 3 did not heterodimerize with RXR α or bind to LXRE in cells (Fig. 5). The conformation of LXR α 3 may be unstable and be influenced by experimental conditions.

Compared with the full length LXR α 1, expression of other LXR α isoforms (LXR α 3, LXR α 4 and LXR α 5; in mice, LXR α 3 and LXR α 4) was diminished in normal tissues (Fig. 2, A and C). Chen et al. reported that LXR α 3 is expressed in lung higher than other tissues, while LXR α 2 is abundant in testis (Chen et al., 2005). In our results, human LXR α 3 was highly expressed in brain, heart, leukocyte, skeletal muscle and ovary, while mouse LXR α 3 was high in lung and spleen (Fig. 2, A and C). Further studies are needed to elucidate how LXR α isoform expression is physiologically regulated and whether there are age, sex and racial differences. Interestingly, relative expression levels were increased in several cell lines (Fig. 2B). Although LXR α isoforms were only weakly expressed in the neuron-derived NT2/D1 and SK-N-SH cells, the relative expression of LXR α 3 was 60% of LXR α 1 levels in NT2/D1 cells. Chen *et al.* reported that LXR α 3 is expressed to relatively high levels in glioma cells (Chen et al., 2005). Since ligand-activated LXR α 1 inhibits cellular proliferation (Blaschke et al., 2004; Fukuchi et al., 2004; Uno et al., 2009), expression of the functional form of LXR α 1 may be repressed in some malignant cells, such as neuron-derived tumors. LXR α 3, LXR α 4 and LXR α 5 are hypomorphic isoforms that lack dominant-negative activity on LXR α 1. It is unlikely that the expression of these isoforms disturbs LXR α 1 function or contributes to the pathogenesis of human diseases, although the possibility remains that they may gain other unidentified functions. Alternatively, isoform expression may be a consequence of dysfunction of splicing and/or pre-mRNA degradation. Pre-mRNA splicing in

mammalian cells is regulated by a ribonucleoprotein complex known as the spliceosome (Wahl et al., 2009). Patterns of alternative splicing vary in cell types and across development likely due to dynamic changes in the spliceosome protein complement. Alternative splicing is linked to various human diseases, including cancer (Cooper et al., 2009). Extra- and intracellular signaling regulates pre-mRNA splicing by modulating the dynamic assembly of the spliceosome components (Shin and Manley, 2004). In addition to splicing regulation, the RNA quality control system also regulates mRNA expression to prevent the production of truncated proteins with dominant-negative or deleterious gain-of-function activities (Chang et al., 2007). The nonsense-mediated mRNA decay system degrades mRNAs carrying premature translation termination codons. The LXR α 5 mRNA contains a stop codon in a novel exon between exon 6 and 7 of LXR α 1 (Fig. 1). LXR α 5 expression was limited in all of the examined human tissues and cell lines (Fig. 2), a finding that may be due to nonsense-mediated mRNA decay. LXR α dysfunction has been implicated in lipid metabolism disorders, autoimmune diseases, atherosclerosis, and cancers (Bensinger et al., 2008; Fukuchi et al., 2004; Tontonoz and Mangelsdorf, 2003; Vedin et al., 2009). RNA quality control mechanisms may lead to preferential LXR α 1 expression and increased LXR α 3, LXR α 4 and LXR α 5 expression could be biomarkers of LXR α -related diseases. T0901317 treatment differently regulated the expression of LXR α -LBD isoforms in cells (Fig. 3), suggesting that LXR α ligand activation influences the expression of alternatively spliced products in a cell type-dependent manner. Further

studies are required to elucidate the role of LXR α in post-transcriptional RNA control.

We created a structural model of LXR α 4 using the crystal structures of related nuclear receptors, such as LXR α 1 and LXR β . The modeling technique used in this study can be applied for analysis of variants of other nuclear receptors. Further functional studies and computer modeling in combination with X-ray crystal structure analysis should be useful in the development of molecularly targeted nuclear receptor therapies.

Acknowledgements

The authors thank members of the Makishima laboratory for technical assistance and helpful comments, Dr. David J. Mangelsdorf of the Howard Hughes Medical Institute and University of Texas Southwestern Medical Center at Dallas for providing $Lxr\alpha^{-/-}/Lxr\beta^{-/-}$ mice, and Dr. Andrew I. Shulman for editorial assistance.

Authorship Contributions

Participated in research design: Endo-Umeda, Fujimori, Naito, Saito, Yamada, and Makishima

Conducted experiments: Endo-Umeda, Uno, Fujimori, and Naito

Contributed new reagents or analytic tools: Endo-Umeda, Jeong, and Miyachi

Performed data analysis: Endo-Umeda, Naito, Saito, Yamagishi, Tokiwa, Yamada, and Makishima

Wrote or contributed to the writing of the manuscript: Endo-Umeda, and Makishima

References

- Adachi R, Shulman AI, Yamamoto K, Shimomura I, Yamada S, Mangelsdorf DJ, and Makishima M (2004) Structural determinants for vitamin D receptor response to endocrine and xenobiotic signals. *Mol Endocrinol* **18**:43-52.
- Bensinger SJ, Bradley MN, Joseph SB, Zelcer N, Janssen EM, Hausner MA, Shih R, Parks JS, Edwards PA, Jamieson BD, and Tontonoz P (2008) LXR signaling couples sterol metabolism to proliferation in the acquired immune response. *Cell* **134**:97-111.
- Blaschke F, Leppanen O, Takata Y, Caglayan E, Liu J, Fishbein MC, Kappert K, Nakayama KI, Collins AR, Fleck E, Hsueh WA, Law RE, and Bruemmer D (2004) Liver X receptor agonists suppress vascular smooth muscle cell proliferation and inhibit neointima formation in balloon-injured rat carotid Arteries. *Circ Res* **95**:e110-123.
- Chandra V, Huang P, Hamuro Y, Raghuram S, Wang Y, Burris TP, and Rastinejad F (2008) Structure of the intact PPAR- γ -RXR- α nuclear receptor complex on DNA. *Nature* **456**:350-356.
- Chang YF, Imam JS, and Wilkinson MF (2007) The nonsense-mediated decay RNA surveillance pathway. *Annu Rev Biochem* **76**:51-74.
- Chen M, Beaven S, and Tontonoz P (2005) Identification and characterization of two alternatively spliced transcript variants of human liver X receptor alpha. *J Lipid*

Res **46**:2570-2579.

Cooper TA, Wan L, and Dreyfuss G (2009) RNA and disease. *Cell* **136**:777-793.

Fukuchi J, Kokontis JM, Hiipakka RA, Chuu C-p, and Liao S (2004) Antiproliferative effect of liver X receptor agonists on LNCaP human prostate cancer cells. *Cancer Res* **64**:7686-7689.

Gampe RT, Montana VG, Lambert MH, Miller AB, Bledsoe RK, Milburn MV, Kliewer SA, Willson TM, and Xu HE (2000) Asymmetry in the PPAR γ /RXR α crystal structure reveals the molecular basis of heterodimerization among nuclear receptors. *Mol Cell* **5**:545-555.

Inaba Y, Yamamoto K, Yoshimoto N, Matsunawa M, Uno S, Yamada S, and Makishima M (2007) Vitamin D₃ derivatives with adamantane or lactone ring side chains are cell type-selective vitamin D receptor modulators. *Mol Pharmacol* **71**:1298-1311.

Ishizawa M, Matsunawa M, Adachi R, Uno S, Ikeda K, Masuno H, Shimizu M, Iwasaki K-i, Yamada S, and Makishima M (2008) Lithocholic acid derivatives act as selective vitamin D receptor modulators without inducing hypercalcemia. *J Lipid Res* **49**:763-772.

Joseph SB, Bradley MN, Castrillo A, Bruhn KW, Mak PA, Pei L, Hogenesch J, O'Connell R M, Cheng G, Saez E, Miller JF, and Tontonoz P (2004) LXR-dependent gene expression is important for macrophage survival and the innate immune response. *Cell* **119**:299-309.

Kaneko E, Matsuda M, Yamada Y, Tachibana Y, Shimomura I, and Makishima M (2003)

Induction of intestinal ATP-binding cassette transporters by a phytosterol-derived liver X receptor agonist. *J Biol Chem* **278**:36091-36098.

Laffitte BA, Joseph SB, Walczak R, Pei L, Wilpitz DC, Collins JL, and Tontonoz P (2001)

Autoregulation of the human liver X receptor α promoter. *Mol Cell Biol* **21**:7558-7568.

Li Y, Bolten C, Bhat BG, Woodring-Dietz J, Li S, Prayaga SK, Xia C, and Lala DS (2002)

Induction of human liver X receptor alpha gene expression via an autoregulatory loop mechanism. *Mol Endocrinol* **16**:506-514.

Lu TT, Makishima M, Repa JJ, Schoonjans K, Kerr TA, Auwerx J, and Mangelsdorf DJ

(2000) Molecular basis for feedback regulation of bile acid synthesis by nuclear receptors. *Mol Cell* **6**:507-515.

Makishima M (2005) Nuclear receptors as targets for drug development: regulation of

cholesterol and bile acid metabolism by nuclear receptors. *J Pharmacol Sci* **97**:177-183.

Noguchi-Yachide T, Aoyama A, Makishima M, Miyachi H, and Hashimoto Y (2007)

Liver X receptor antagonists with a phthalimide skeleton derived from thalidomide-related glucosidase inhibitors. *Bioorg Med Chem Lett* **17**:3957-3961.

Ou J, Tu H, Shan B, Luk A, DeBose-Boyd RA, Bashmakov Y, Goldstein JL, and Brown

MS (2001) Unsaturated fatty acids inhibit transcription of the sterol regulatory

element-binding protein-1c (SREBP-1c) gene by antagonizing ligand-dependent activation of the LXR. *Proc Natl Acad Sci USA* **98**:6027-6032.

Peet DJ, Turley SD, Ma W, Janowski BA, Lobaccaro JM, Hammer RE, and Mangelsdorf DJ (1998) Cholesterol and bile acid metabolism are impaired in mice lacking the nuclear oxysterol receptor LXR α . *Cell* **93**:693-704.

Repa JJ and Mangelsdorf DJ (2002) The liver X receptor gene team: potential new players in atherosclerosis. *Nat Med* **8**:1243-1248.

Repa JJ, Turley SD, Lobaccaro JA, Medina J, Li L, Lustig K, Shan B, Heyman RA, Dietschy JM, and Mangelsdorf DJ (2000) Regulation of absorption and ABC1-mediated efflux of cholesterol by RXR heterodimers. *Science* **289**:1524-1529.

Rosenfeld MG, Lunyak VV, and Glass CK (2006) Sensors and signals: a coactivator/corepressor/epigenetic code for integrating signal-dependent programs of transcriptional response. *Genes Dev* **20**:1405-1428.

Schultz JR, Tu H, Luk A, Repa JJ, Medina JC, Li L, Schwendner S, Wang S, Thoolen M, Mangelsdorf DJ, Lustig KD, and Shan B (2000) Role of LXRs in control of lipogenesis. *Genes Dev* **14**:2831-2838.

Shin C, and Manley JL (2004) Cell signalling and the control of pre-mRNA splicing. *Nat Rev Mol Cell Biol* **5**:727-738.

Spencer TA, Li D, Russel JS, Collins JL, Bledsoe RK, Consler TG, Moore LB, Galardi

- CM, McKee DD, Moore JT, Watson MA, Parks DJ, Lambert MH, and Willson TM (2001) Pharmacophore analysis of the nuclear oxysterol receptor LXR α . *J Med Chem* **44**:886-897.
- Svensson S, Ostberg T, Jacobsson M, Norstrom C, Stefansson K, Hallen D, Johansson IC, Zachrisson K, Ogg D, and Jendeberg L (2003) Crystal structure of the heterodimeric complex of LXR α and RXR β ligand-binding domains in a fully agonistic conformation. *EMBO J* **22**:4625-4633.
- Tontonoz P and Mangelsdorf DJ (2003) Liver X receptor signaling pathways in cardiovascular disease. *Mol Endocrinol* **17**:985-993.
- Uno S, Endo K, Jeong Y, Kawana K, Miyachi H, Hashimoto Y, and Makishima M (2009) Suppression of β -catenin signaling by liver X receptor ligands. *Biochem Pharmacol* **77**:186-195.
- Valledor AF, Hsu L-C, Ogawa S, Sawka-Verhelle D, Karin M, and Glass CK (2004) Activation of liver X receptors and retinoid X receptors prevents bacterial-induced macrophage apoptosis. *Proc Natl Acad Sci USA* **101**:17813-17818.
- Vedin L-L, Lewandowski SA, Parini P, Gustafsson J-A, and Steffensen KR (2009) The oxysterol receptor LXR inhibits proliferation of human breast cancer cells. *Carcinogenesis* **30**:575-579.
- Wahl MC, Will CL, and Luhrmann R (2009) The spliceosome: design principles of a

dynamic RNP machine. *Cell* **136**:701-718.

Williams S, Bledsoe RK, Collins JL, Boggs S, Lambert MH, Miller AB, Moore J, McKee

DD, Moore L, Nichols J, Parks D, Watson M, Wisely B, and Willson TM (2003)

X-ray crystal structure of the liver X receptor β ligand binding domain: regulation

by a histidine-tryptophan switch. *J Biol Chem* **278**:27138-27143.

Willy PJ, Umesono K, Ong ES, Evans RM, Heyman RA, and Mangelsdorf DJ (1995)

LXR, a nuclear receptor that defines a distinct retinoid response pathway. *Genes*

Dev **9**:1033-1045.

Yoshikawa T, Shimano H, Amemiya-Kudo M, Yahagi N, Hasty AH, Matsuzaka T,

Okazaki H, Tamura Y, Iizuka Y, Ohashi K, Osuga J, Harada K, Gotoda T, Kimura

S, Ishibashi S, and Yamada N (2001) Identification of liver X receptor-retinoid X

receptor as an activator of the sterol regulatory element-binding protein 1c gene

promoter. *Mol Cell Biol* **21**:2991-3000.

Footnote

This work was supported in part by the Ministry of Education, Culture, Sports, Science, and Technology of Japan [Grant-in-Aid for Scientific Research on Priority Areas 18077005] (to M.M.).

Current address of Kenji Yamagishi: Department of Chemical Biology and Applied Chemistry, College of Engineering, Nihon University, 1 Nakagawara, Tokusada, Tamura-machi, Koriyama, Fukushima 963-8642, Japan

Legends for Figures

Fig. 1. LXR α -LBD isoforms. (A) Human LXR α gene (GenBank accession number NC_000011), LXR α 1 mRNA (GenBank accession number NM_005693), and LXR α 1 protein (GenBank accession number NP_005684). (B) Alternative splicing that generates LXR α -LBD isoforms. (C) Sequence alignment of LXR α -LBD isoforms. Exons that encode the corresponding amino acids are shown and the exon numbers are as reported by Chen et al. (Chen et al., 2005). Bars and arrows indicate helices (H) and β -sheets (S), respectively.

Fig.2. Differential expression of human and mouse LXR α isoforms. (A) Real-time quantitative reverse transcription-PCR analysis of LXR α isoform expression in a human tissue cDNA panel. Repeated experiment showed similar results. (B, C) Real-time quantitative reverse transcription-PCR analysis of LXR α isoform expression in several human cell lines (B) and in several mouse tissues (C). (C) LXR α 3 and LXR α 4 are expressed weaker than LXR α 1 (left). LXR α 3 and LXR α 4 expression is compared in wild-type mice (WT; middle) and Lxr $\alpha^{-/-}$ /Lxr $\beta^{-/-}$ mice (Lxr $^{-/-}$; right). The values represent means \pm SD of triplicate assays.

Fig. 3. Western blotting analysis of LXR α isoforms. (A) Expression of LXR α 1, LXR α 3 and LXR α 4 proteins is observed in HaCaT cells. Long and short exposures are shown in

upper and lower panels, respectively. (B) HepG2 cells also express LXR α 1, LXR α 3 and LXR α 4 proteins. Cells were transfected with control siRNA, LXR α -siRNA-1, LXR α -siRNA-2, or LXR α / β -siRNA for 48 hours. Nuclear proteins (30 μ g) were immunoblotted with anti-LXR α antibody.

Fig. 4. Effects of an LXR ligand on mRNA expression of LXR α isoforms. Cells were treated with ethanol (EtOH) or 1 μ M T0901317 for 24 hours. *, $p < 0.05$; **, $p < 0.01$; ***, $p < 0.001$ compared with ethanol control. The values represent the means \pm S.D. of triplicate assays.

Fig. 5. Transactivation, transrepression and RXR heterodimerization of LXR α isoforms.

(A) Immunoblot analysis of LXR α isoforms expressed in HEK293 cells. Cells were transfected with pFLAG-CMV2 control (Cont), pFLAG-CMV2-VP16 (VP16-Cont), pFLAG-CMV-LXR α isoform, or pFLAG-CMV2-VP16-LXR α isoform. LXR α proteins were detected with anti-FLAG antibody. Each lane was loaded with 20 μ g of proteins. (B) Transactivation of LXR α isoforms on an LXRE reporter by T0901317. HEK293 cells were transfected with pFLAG-CMV2 control (-), pFLAG-CMV2-LXR α 1 (α 1), pFLAG-CMV2-LXR α 3 (α 3), pFLAG-CMV2-LXR α 4 (α 4), or pFLAG-CMV2-LXR α 5 (α 5), and (rCyp7a-DR4)x3-tk-LUC, and were treated with ethanol (EtOH), 10 nM, 30 nM, or 100 nM T0901317. (C) Effects of constitutively active LXR α isoforms on LXRE.

HEK293 cells were transfected with pFLAG-CMV2-VP16 control (-), pFLAG-CMV2-VP16-LXR α 1 (α 1), pFLAG-CMV2-VP16-LXR α 3 (α 3), pFLAG-CMV2-VP16-LXR α 4 (α 4), or pFLAG-CMV2-VP16-LXR α 5 (α 5), and treated as in (B). (D) Repressive activity of LXR α isoforms on β -catenin transactivation. HEK293 cells were transfected with pFLAG-CMV2 control (-), pFLAG-CMV2-LXR α 1 (α 1), pFLAG-CMV2-LXR α 3 (α 3), pFLAG-CMV2-LXR α 4 (α 4), or pFLAG-CMV2-LXR α 5 (α 5), in combination with pCMX control (-) or pCMX- β -catenin-MT (+), and TOP-GLOW, and treated with ethanol (EtOH) or 100 nM T0901317. (E) Interaction of VP16-LXR α isoforms with GAL4 chimera of RXR α -LBD. Cells were transfected with pCMX-GAL4 control or pCMX-GAL4-RXR α in combination with pFLAG-CMV2-VP16 control (-), pFLAG-CMV2-VP16-LXR α 1 (α 1), pFLAG-CMV2-VP16-LXR α 3 (α 3), pFLAG-CMV2-VP16-LXR α 4 (α 4), or pFLAG-CMV2-VP16-LXR α 5 (α 5), and MH100(UAS)x4-tk-LUC, and were treated with ethanol control (EtOH) or 100 nM T0901317. (F) Interaction of GAL4 chimera of LXR α -LBDs with VP16-RXR α . Cells were transfected with pCMX-GAL4 control (-), pCMX-GAL4-LXR α 1 (α 1), pCMX-GAL4-LXR α 3 (α 3), pCMX-GAL4-LXR α 4 (α 4), or pCMX-GAL4-LXR α 5 (α 5) in combination with pCMX-VP16 control or pCMX-VP16-RXR α , and MH100(UAS)x4-tk-LUC, and were treated as in (E). The values represent the means \pm S.D. of triplicate assays.

Fig. 6. LXR α 1, but not LXR α 3, LXR α 4 or LXR α 5, binds to LXREs. (A) LXREa from the mouse SREBP-1c were labeled and incubated with LXR α 1 and/or RXR α proteins. Preincubation with anti-LXR α antibody (1, 5 or 10 μ g) and unlabeled LXREa probes (0.01, 0.1 or 1 μ M) was performed for supershift and competition, respectively. (B) LXR α 1, but not LXR α 3, LXR α 4 or LXR α 5, in combination with RXR α binds to LXREa from SREBP-1c. Treatment with 1 μ M T0901317 does not affect a complex formation. (C) EMSAs using LXREs from the mouse SREBP-1c promoter (LXREa and LXREb), the rat CYP7A promoter and the rat fatty acid synthase (FAS) promoter.

Fig. 7. Effects of GW3965, oxysterols and fatty acids on transactivation of LXR α isoforms. (A) LXR agonists, GW3965, 24(S),25-epoxycholesterol, and 22(R)-hydroxycholesterol, induce activation of LXR α 1 and LXR α 4 but not LXR α 3 or LXR α 5. LXR α antagonists, 22(S)-hydroxycholesterol, arachidonic acid, and linolenic acid, are not effective on transactivation of LXR α isoforms. HEK293 cells were transfected as in Fig. 5B and treated with ethanol (EtOH), GW3965 (GW), 24(S),25-epoxycholesterol (EC), 22(R)-hydroxycholesterol (22R), 22(S)-hydroxycholesterol (22S), arachidonic acid (AA), or linolenic acid (LA). (B) LXR α antagonists suppress transactivation of LXR α 1 and LXR α 4 induced by GW3965 and 24(S),25-epoxycholesterol. HEK293 cells were transfected as in Fig. 5B and treated with 1 μ M GW3965 (GW) or 10 μ M 24(S),25-epoxycholesterol (EC) in combination

with ethanol (EtOH), 22(*S*)-hydroxycholesterol (22S) or arachidonic acid (AA). The values represent means \pm SD of triplicate assays.

Fig. 8. Interaction of LXR α isoforms with cofactors. Interaction of LXR α isoforms with coactivators, SRC-1 (A) and DRIP205 (B). Cells were transfected with pFLAG-CMV2-VP16 control (-), pFLAG-CMV2-VP16-LXR α 1 (α 1), pFLAG-CMV2-VP16-LXR α 3 (α 3), pFLAG-CMV2-VP16-LXR α 4 (α 4), or pFLAG-CMV2-VP16-LXR α 5 (α 5), in combination with pCMX-GAL4-SRC-1 (A) or pCMX-GAL4-DRIP205, and MH100(UAS)x4-tk-LUC, and were treated with ethanol control (EtOH) or 100 nM T0901317. Cells were cotransfected without (left panel) or with pCMX-RXR α (right panel). (C) Interaction of LXR α isoforms with corepressors. Cells were transfected with pFLAG-CMV2-VP16 control (-), pFLAG-CMV2-VP16-LXR α 1 (α 1), pFLAG-CMV2-VP16-LXR α 3 (α 3), pFLAG-CMV2-VP16-LXR α 4 (α 4), or pFLAG-CMV2-VP16-LXR α 5 (α 5), in combination with pCMX-RXR α , pCMX-GAL4-N-CoR or pCMX-GAL4-SMRT, and MH100(UAS)x4-tk-LUC, and were treated as in (A). The values represent the means \pm S.D. of triplicate assays.

Fig. 9. Effects of overexpression of LXR α isoforms on LXR α 1 transactivation and expression of LXR target genes. (A) Transactivation activity of LXR α 1 is not inhibited

by overexpression of LXR α 3 or LXR α 4, but is inhibited by LXR α 5. HEK293 cells were transfected with 0.1 ng of pFLAG-CMV2 control (-) or pFLAG-CMV2-LXR α 1 (+), in combination with 0 (-), 15 (+), 30 (++), or 60 ng (+++) of pFLAG-CMV2-LXR α 3 (α 3), pFLAG-CMV2-LXR α 4 (α 4), or pFLAG-CMV2-LXR α 5 (α 5), and (rCyp7a-DR4)x3-tk-LUC, and were treated with ethanol (EtOH), 10 nM, 30 nM, or 100 nM T0901317. The total amounts of plasmids were adjusted by addition of pFLAG-CMV2 control vector. (B) SW480 cells were transfected with 2.5 μ g of control plasmid (-), pFLAG-CMV2-LXR α 1 (α 1), pFLAG-CMV2-LXR α 3 (α 3), pFLAG-CMV2-LXR α 4 (α 4), or pFLAG-CMV2-LXR α 5 (α 5), and were treated with ethanol (EtOH) or 30 nM T0901317 for 24 hours. Endogenous SREBP-1c and ABCA1 mRNA levels were determined by quantitative real-time PCR analysis. Effects of T0901317 on induction of these genes were significant in all transfection experiments. *, $p < 0.05$; ***, $p < 0.001$ compared with control plasmid. (C) Combination of LXR α 5 cotransfection and LXR α antagonist treatment exhibits additive effects on inhibition of agonist-induced LXR α 1 activation. HEK293 cells were transfected with 0.1 ng of pFLAG-CMV2-LXR α 1 (+) in combination with 0 (-), 40 (+), or 60 ng (++) of pFLAG-CMV2-LXR α 5 (α 5), and (rCyp7a-DR4)x3-tk-LUC, and were treated with 1 μ M GW3965 (GW) or 10 μ M 24(S),25-epoxycholesterol (EC) in combination with ethanol (EtOH), 22(S)-hydroxycholesterol (22S) or arachidonic acid (AA). The values represent means \pm SD of triplicate assays.

Fig. 10. Structural model of LXR α 4. (A) Model of LXR α 4-LBD docked with T0901317 (model M2) was created by automatic selection of LXR β -LBD/24(S),25-epoxycholesterol complex (Protein Data Bank code 1p8d) as a template and optimization of the complex docked with T0901317 whose structure was extracted from the LXR α -LBD/RXR β -LBD/T0901317 complex (Protein Data Bank code 1uhl). (B) Model of LXR α 4/RXR heterodimer (model M3) was created by overlying the liganded model, in which LXR β in LXR β -LBD/24(S),25-epoxcholesterol (Protein Data Bank code 1p8d) was replaced with LXR α 4, with the LXR α -LBD/RXR β -LBD/T0901317 (Protein Data Bank code 1uhl). (C) In model M4, the SRC-1 coactivator peptide was placed at LXR α 4 in the same place as LXR α 1. H, helix.

Table 1. Primer sequences for real-time quantitative reverse transcription-PCR (human)

Gene	Sequence (5' to 3')	Amplicon size (bp)
LXR α 1	CTG CGA TCG AGG TGA TGC TT (fw) ACT ACG GCT CAA ACG GAA C (rev)	197
LXR α 3	TGA AGC GGC AAG AGG AGG AA (fw) AGC TCA GTG CCA CTA CGA AG (rev)	166
LXR α 4	CGT TTG AGG TTT GCT GCT TG (fw) ACT ACG GCT CAA ACG GAA C (rev)	233
LXR α 5	CTG CGA TCG AGG TGA TGC TT (fw) GTT AGT ACC GAG TTA CGT CG (rev)	155
GAPDH	ACT TCG CTC AGA CAC CAT GG (fw) GGG AAG TAA CTG GAG TTG ATG (rev)	139

GAPDH, glyceraldehyde-3-phosphate dehydrogenase.

fw, forward primer; rev, reverse primer.

Table 2. Primer sequences for real-time quantitative reverse transcription-PCR (mouse)

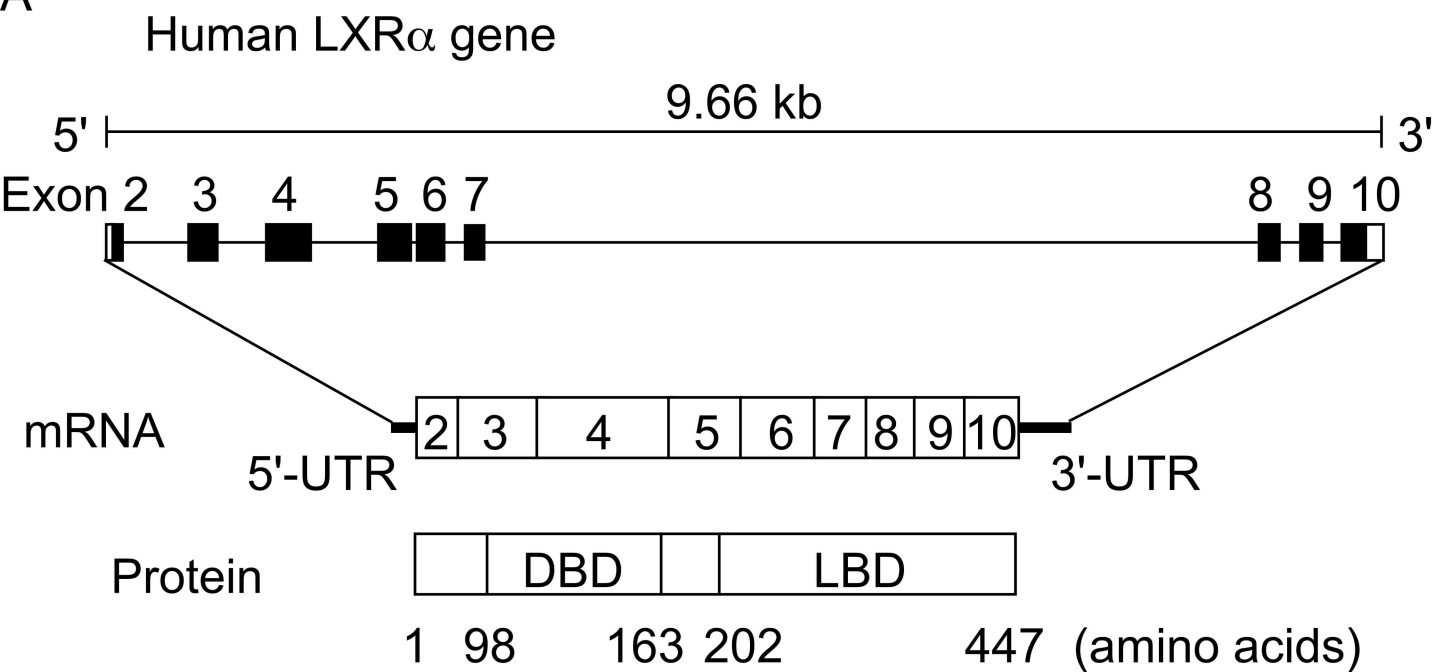
Gene	Sequence (5' to 3')	Amplicon size (bp)
LXR α 1	CTG CAA TCG AGG TCA TGC TT (fw) GCA GAG CAA ACT CAG CAT CA (rev)	198
LXR α 3	TGA AGC GGC AAG AAG AGG AA (fw) CTC TCC AGA AGC ATG ACC GT (rev)	189
LXR α 4	CCT GTC TGA AAG ATG CTG CT (fw) GCA GAG CAA ACT CAG CAT CA (rev)	216
GAPDH	TGC ACC ACC AAC TGC TTA G (fw) GAT GCA GGG ATG ATG TTC (rev)	176

GAPDH, glyceraldehyde-3-phosphate dehydrogenase.

fw, forward primer; rev, reverse primer.

Fig. 1, A and B

A



B

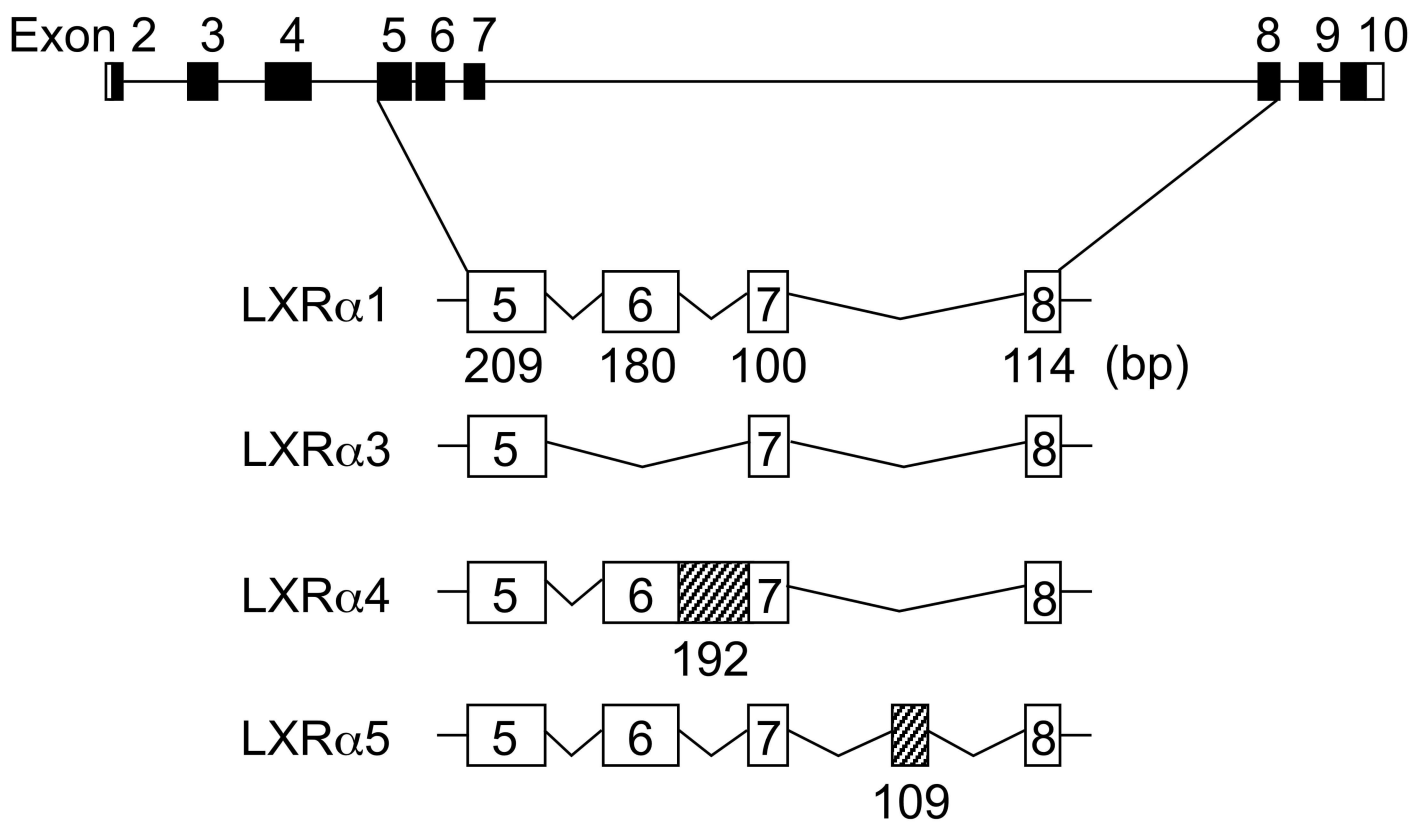


Fig. 1, C

C

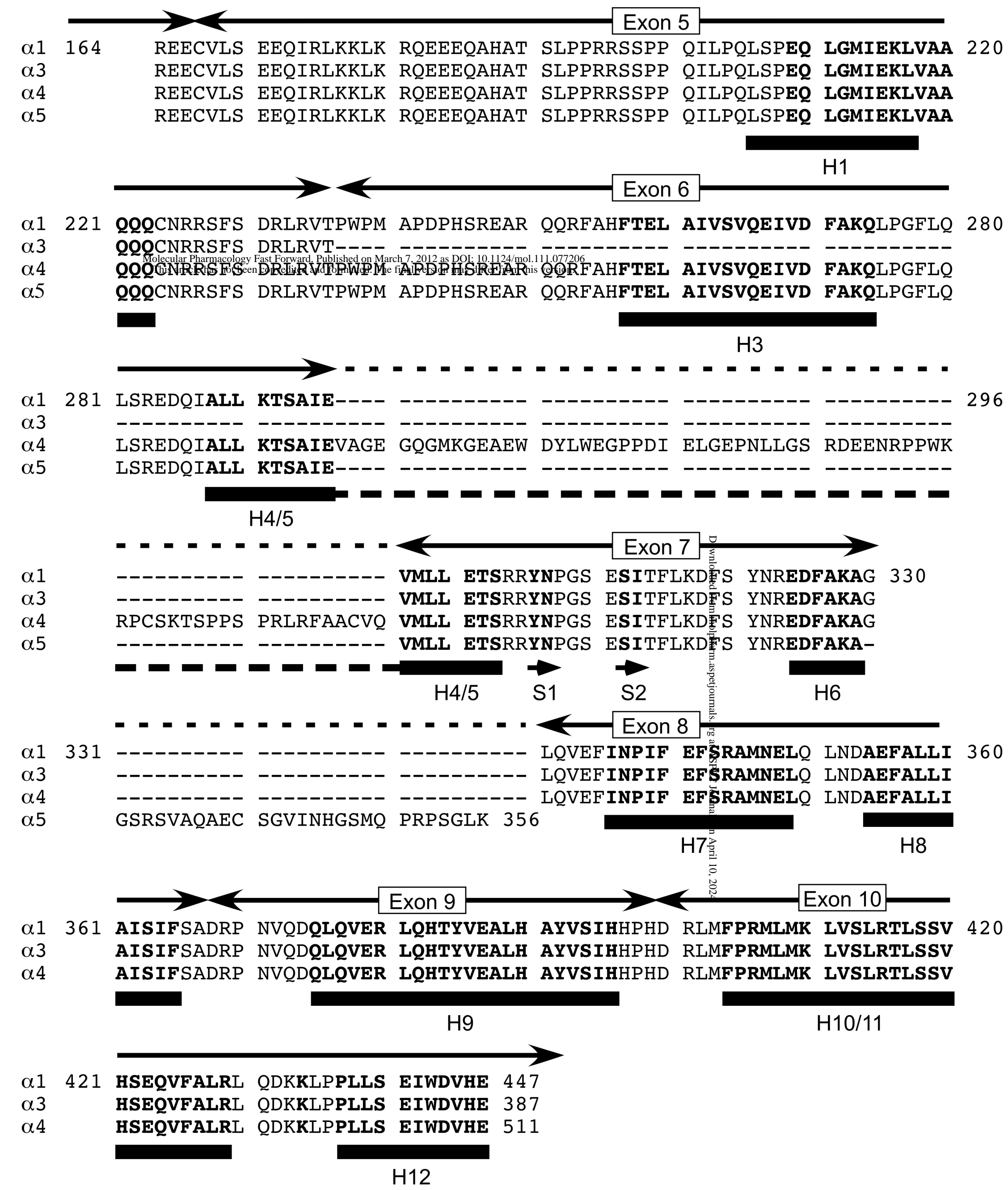
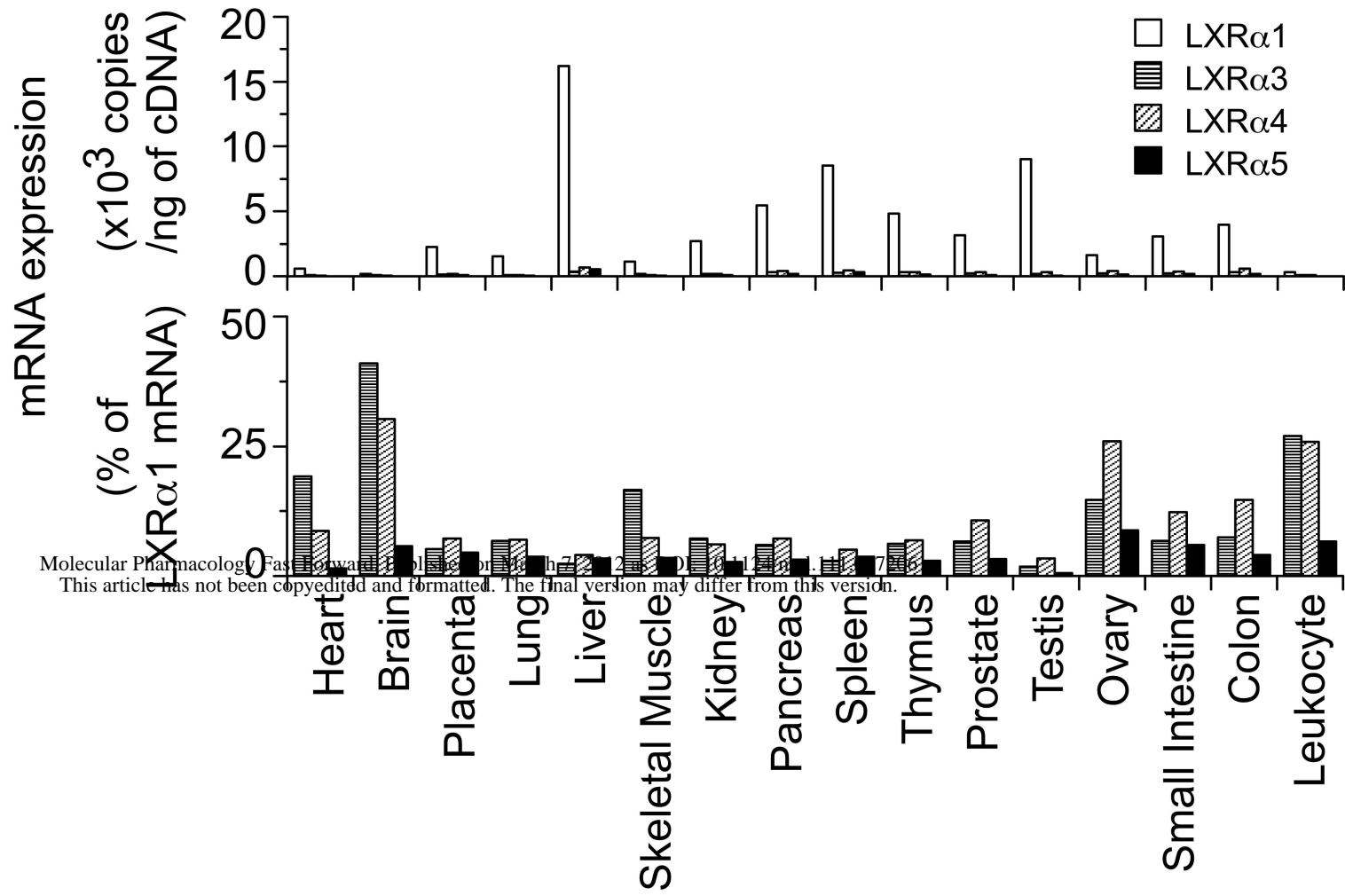
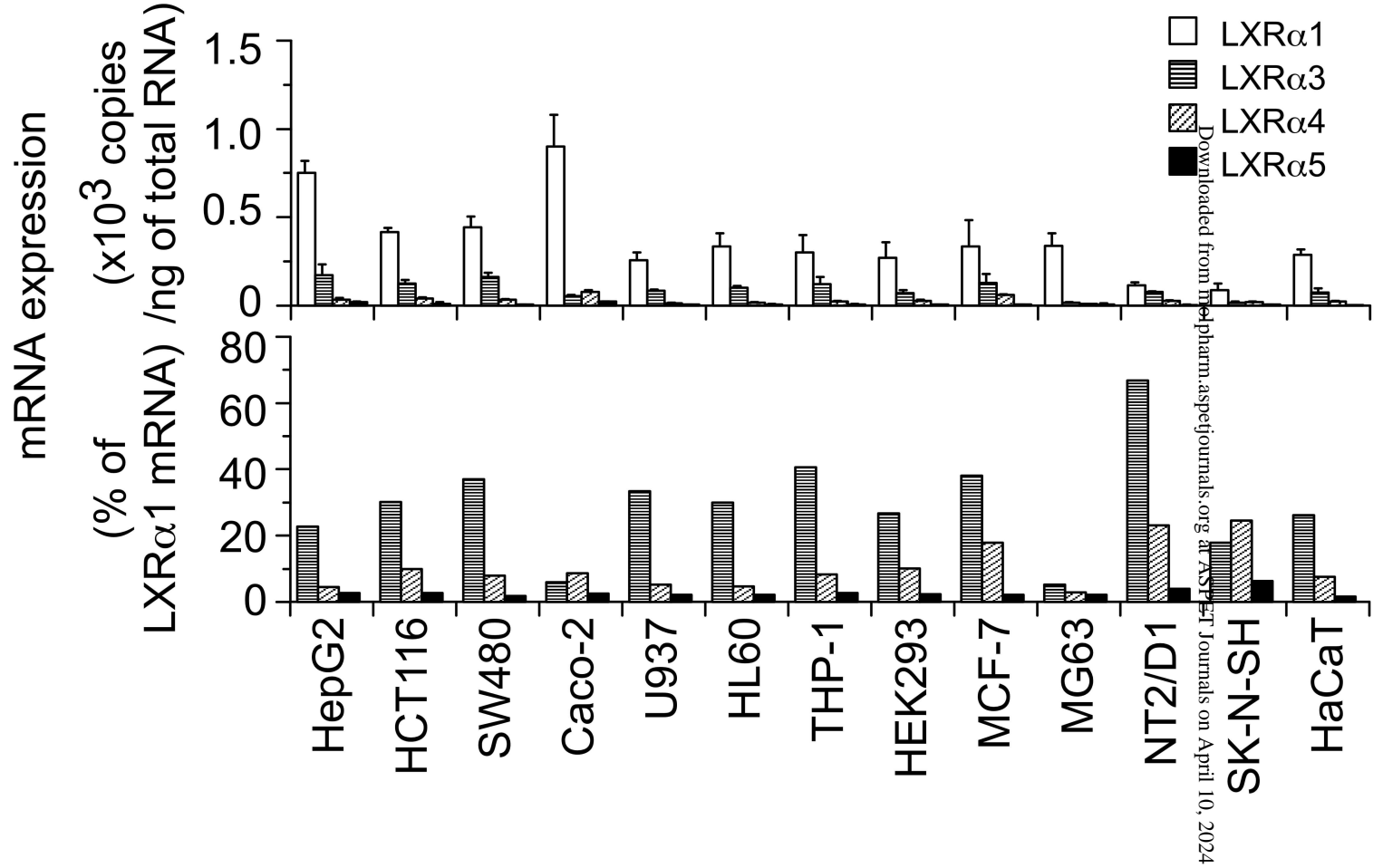


Fig. 2

A



B



C

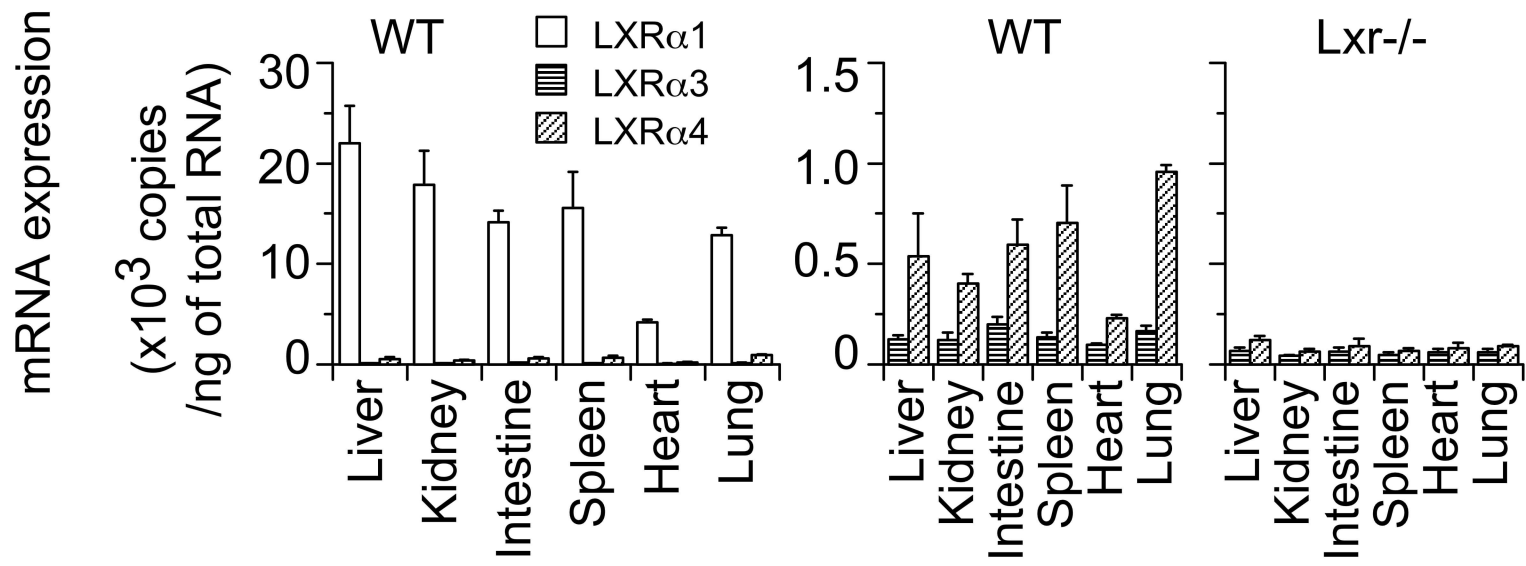
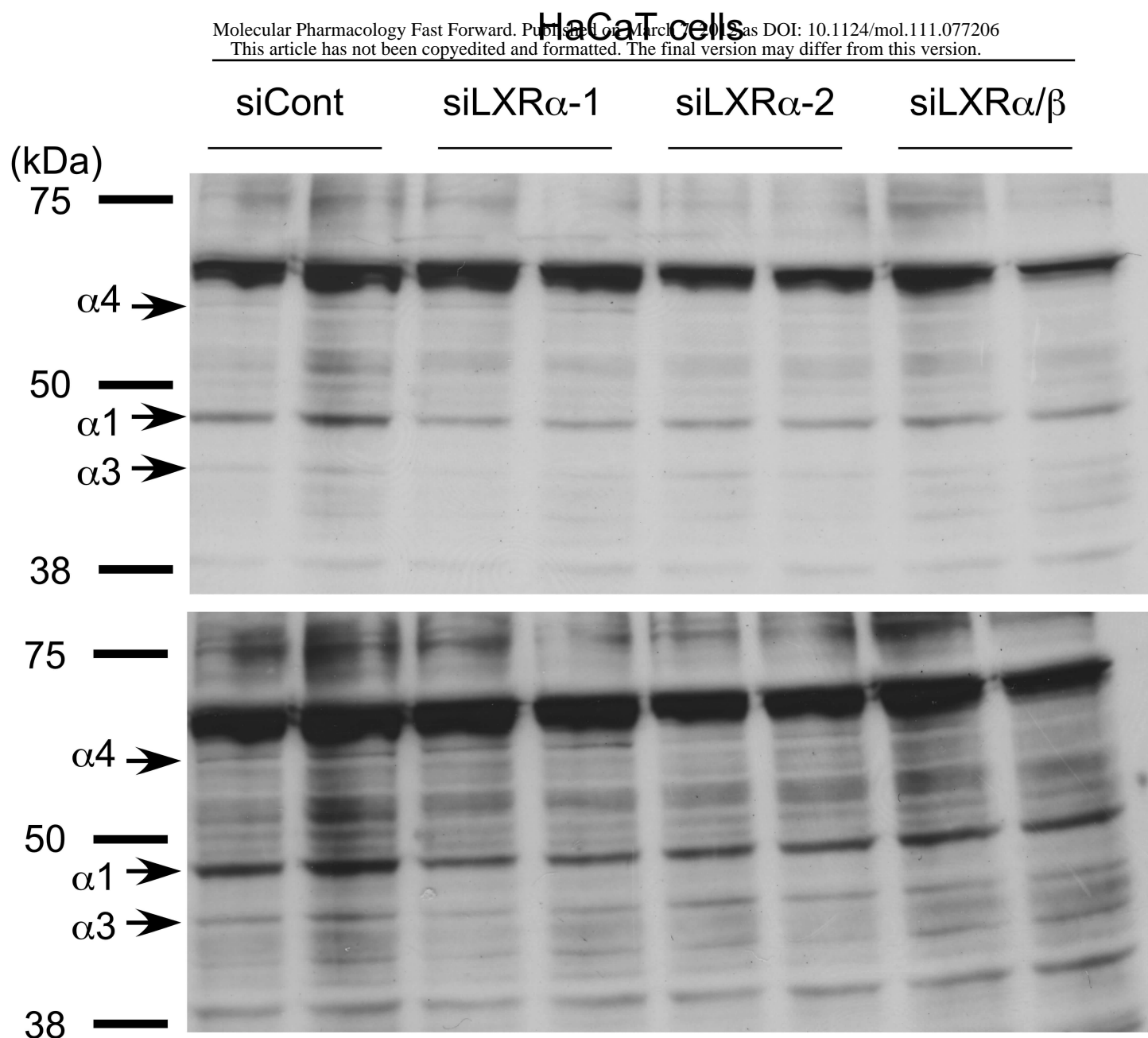


Fig. 3

A



B

HepG2 cells

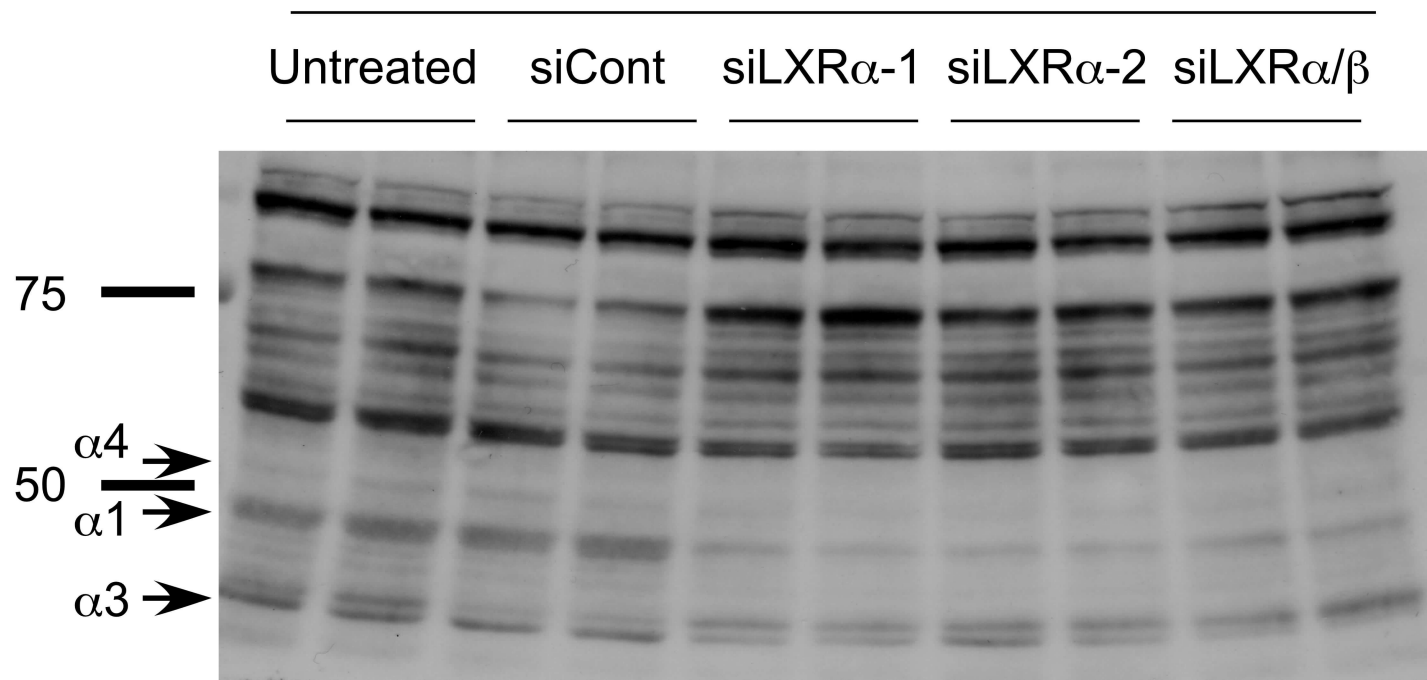


Fig. 4

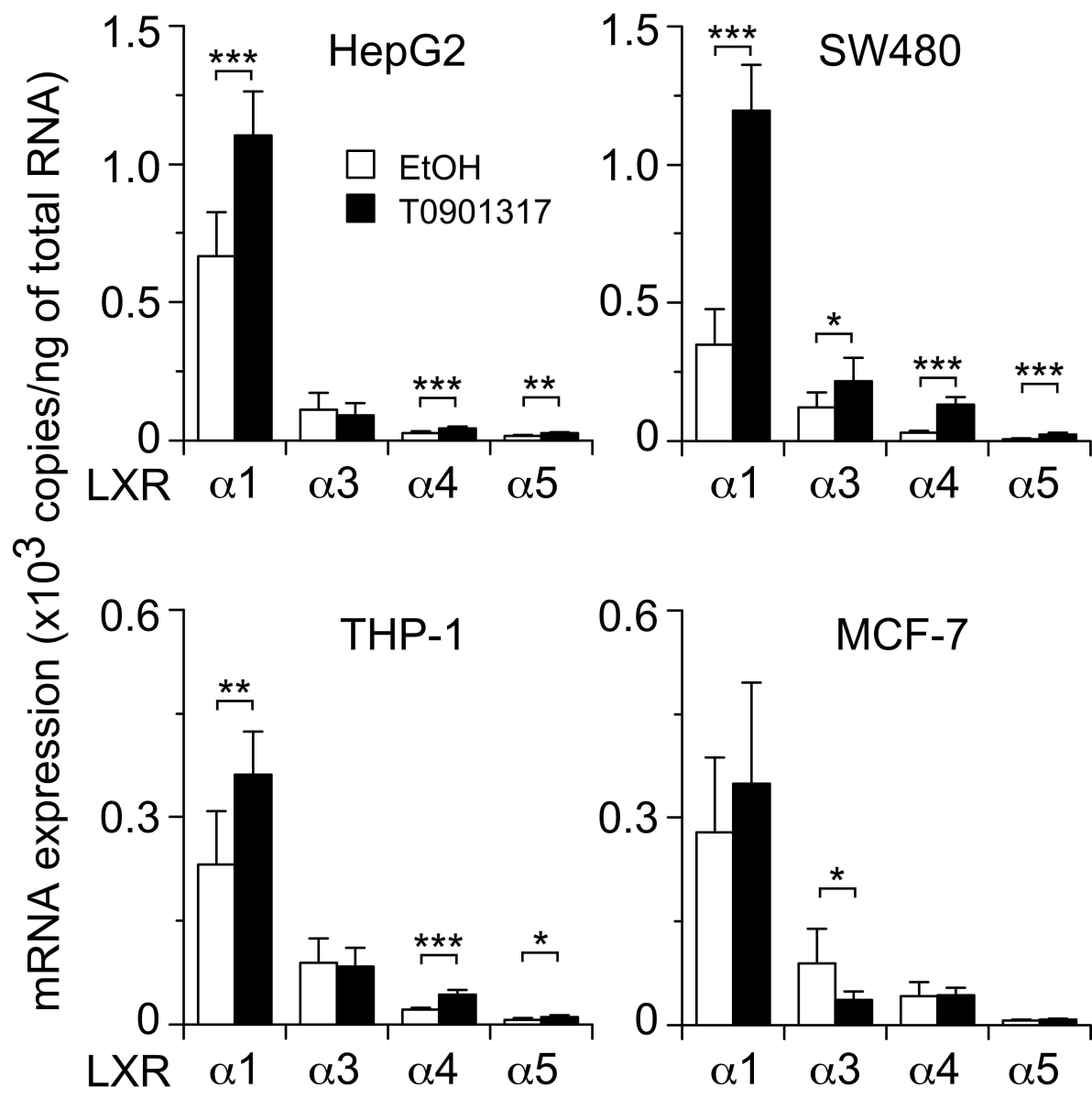


Fig. 5, A, B and C

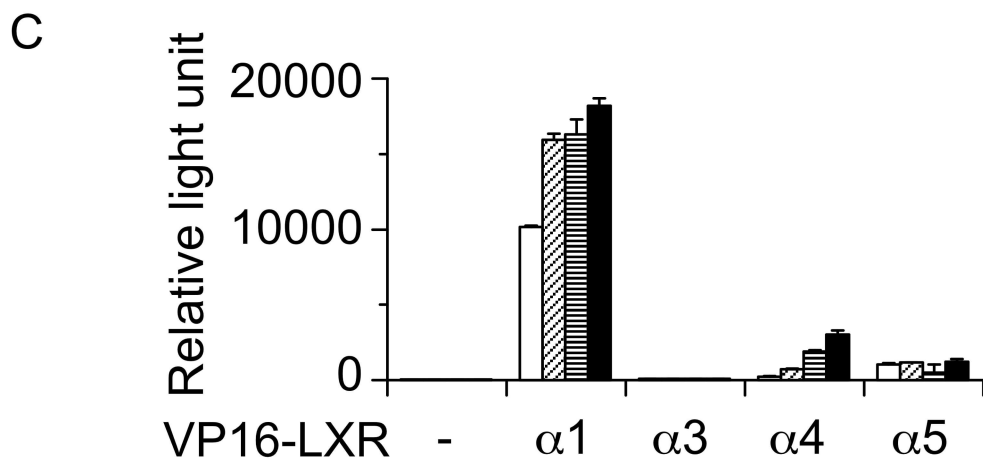
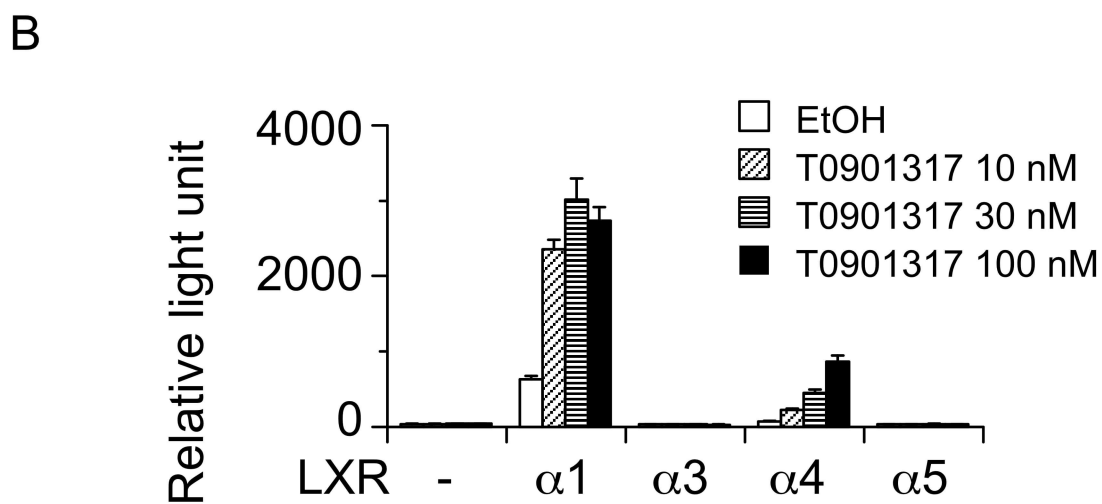
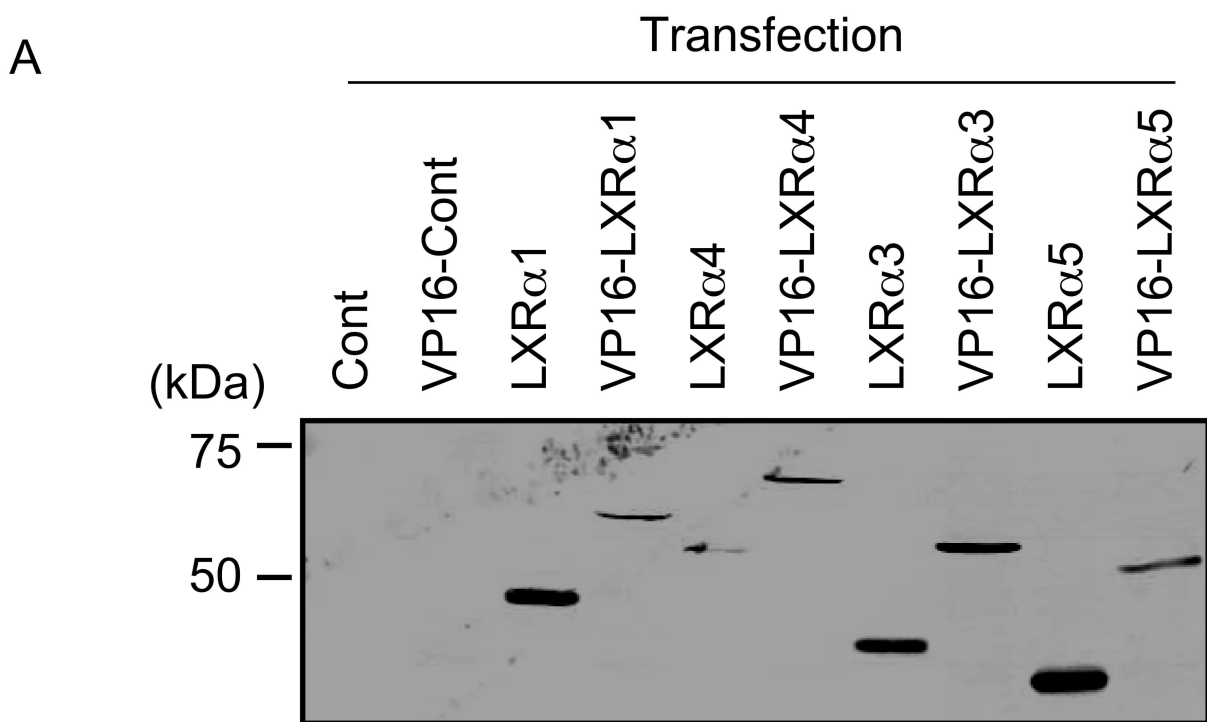
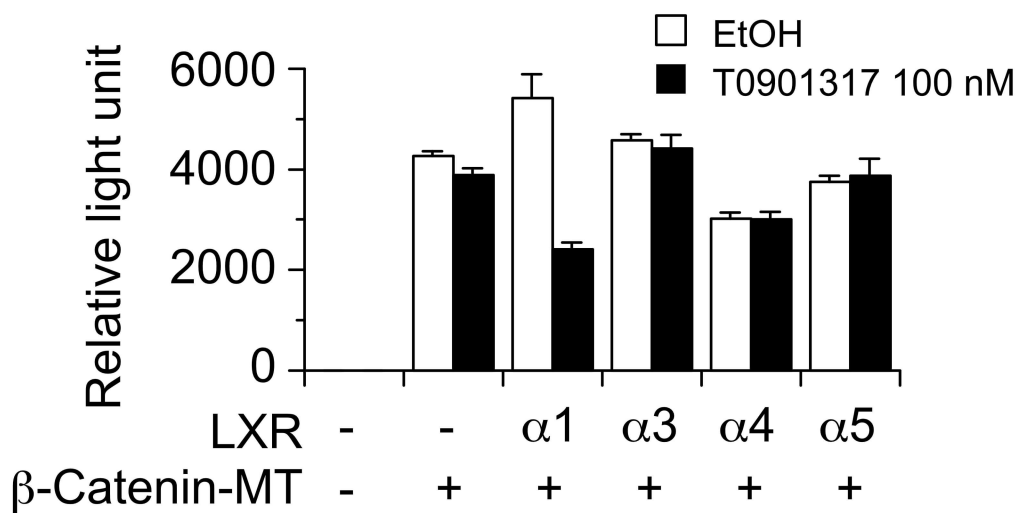
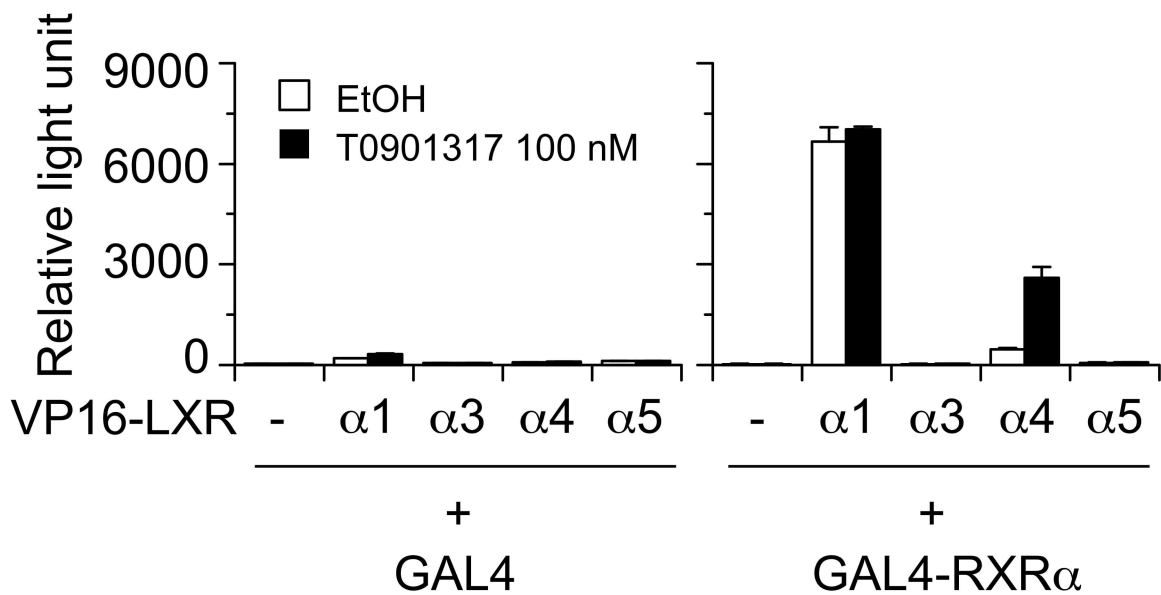


Fig. 5, D, E and F

D



E



F

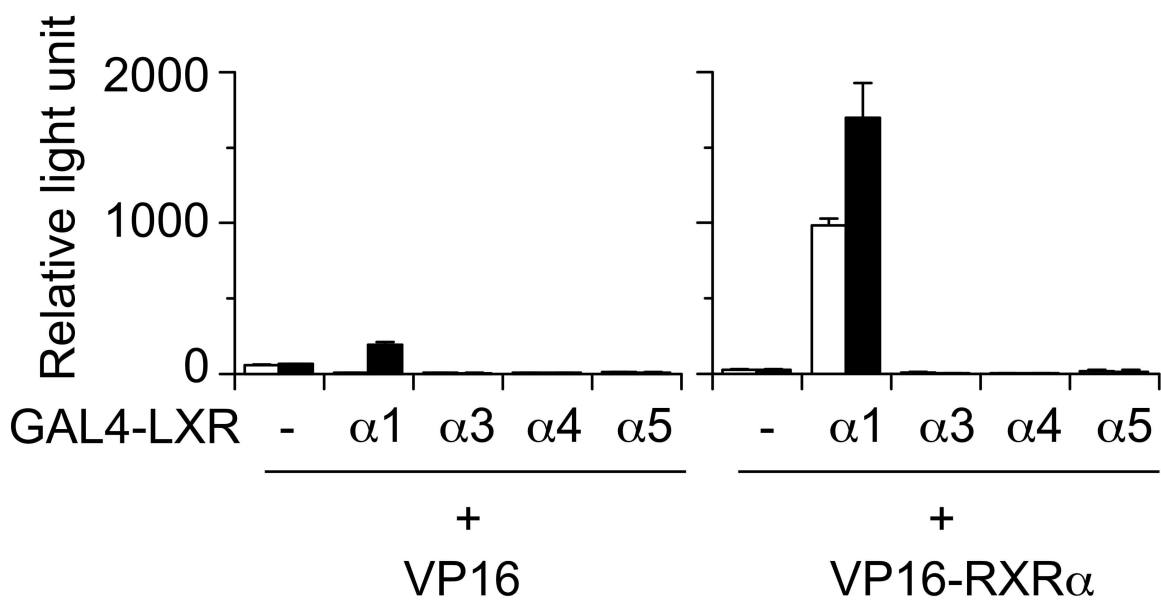
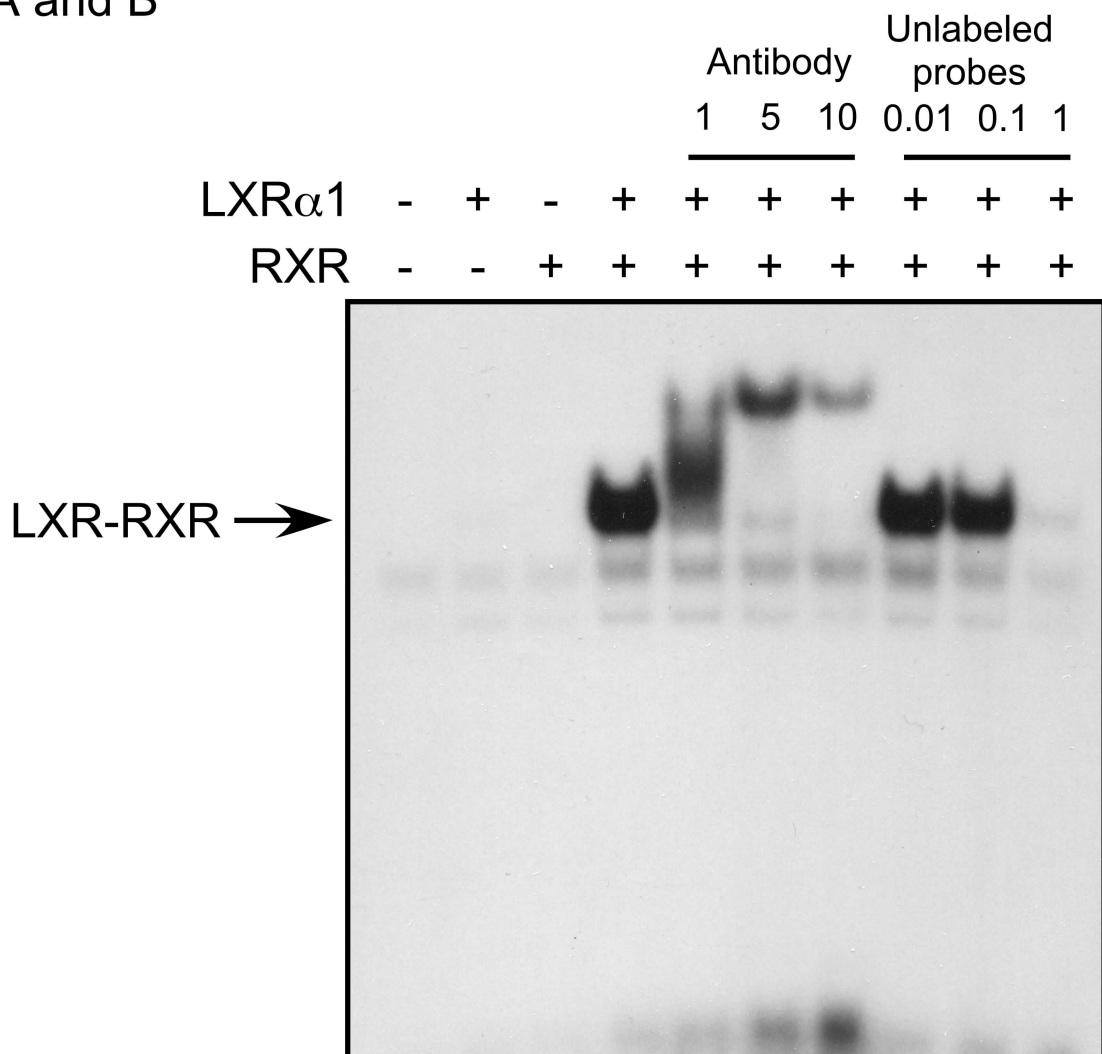


Figure 6, A and B

A



B

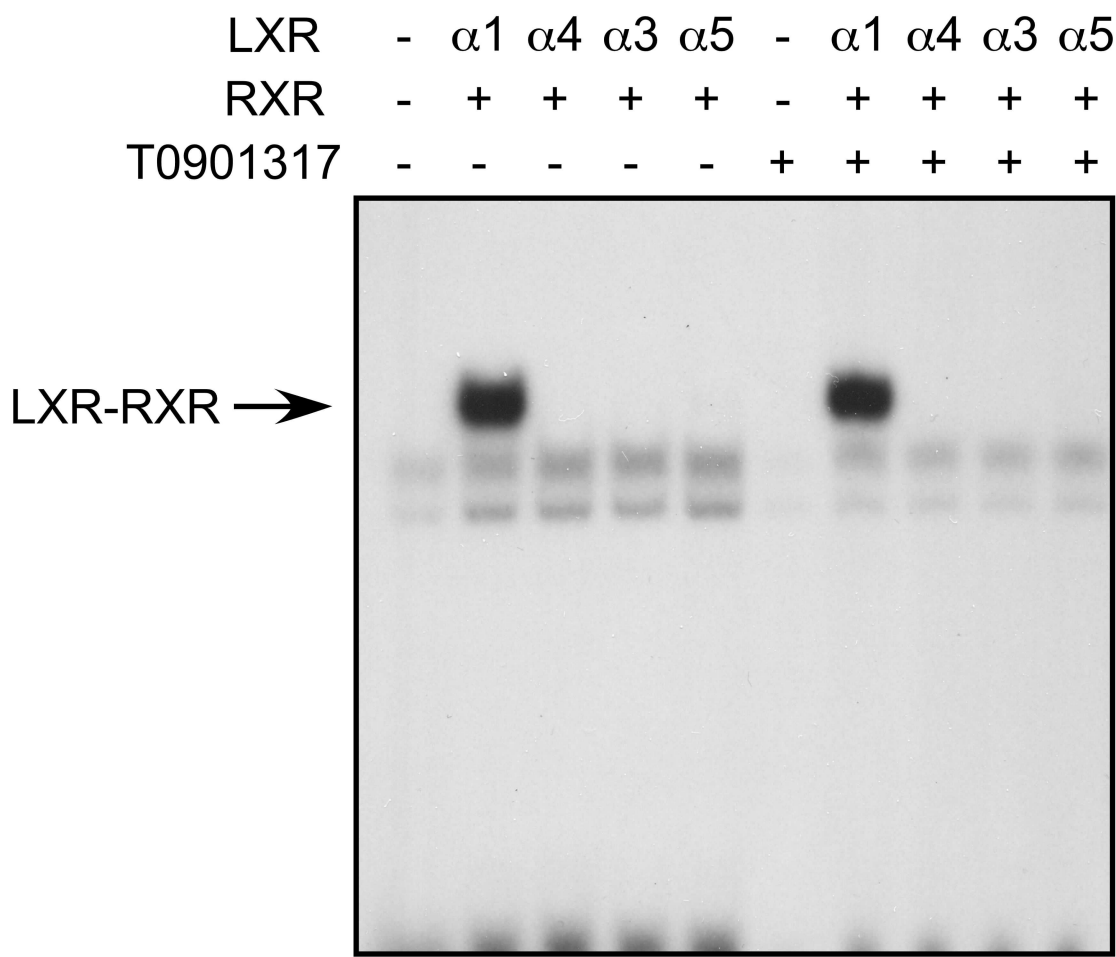


Figure 6, C

C

Probes	SREBP-1c						CYP7A			FAS		
	LXREa			LXREb								
LXR	-	$\alpha 1$	$\alpha 5$	-	$\alpha 1$	$\alpha 5$	-	$\alpha 1$	$\alpha 5$	-	$\alpha 1$	$\alpha 5$
RXR	-	+	+	-	+	+	-	+	+	-	+	+

LXR-RXR →

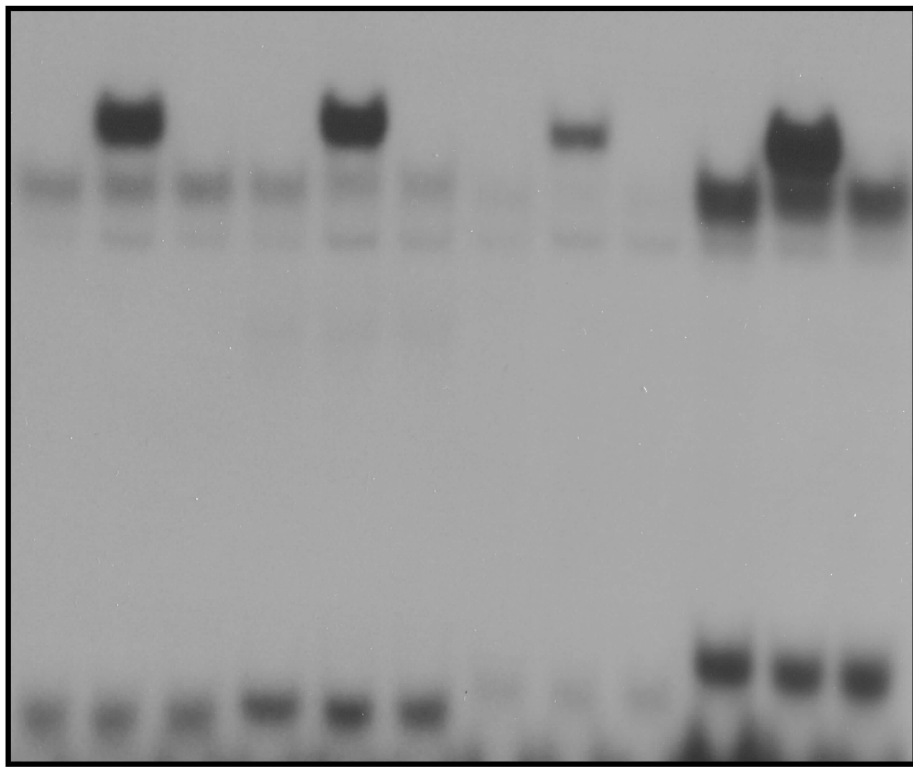
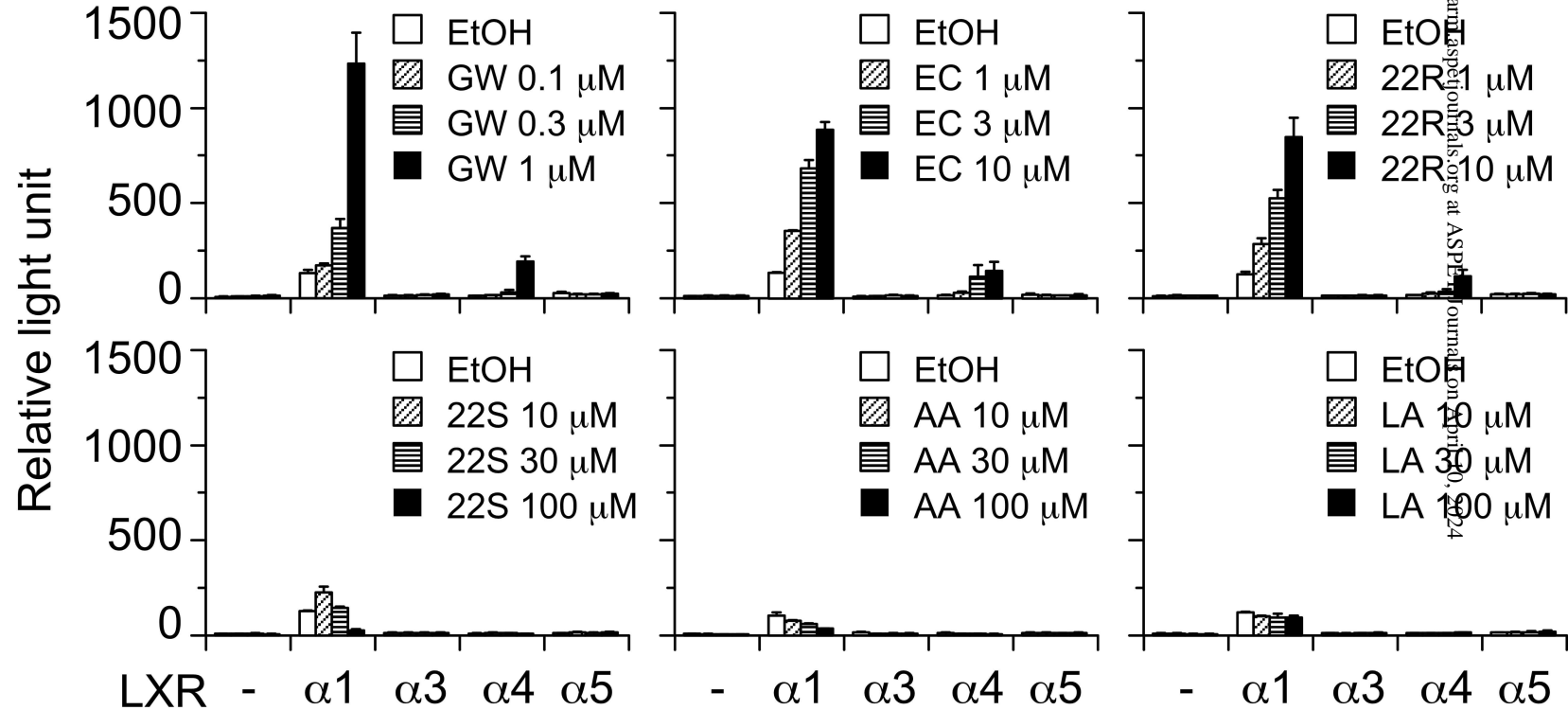


Fig. 7

A



B

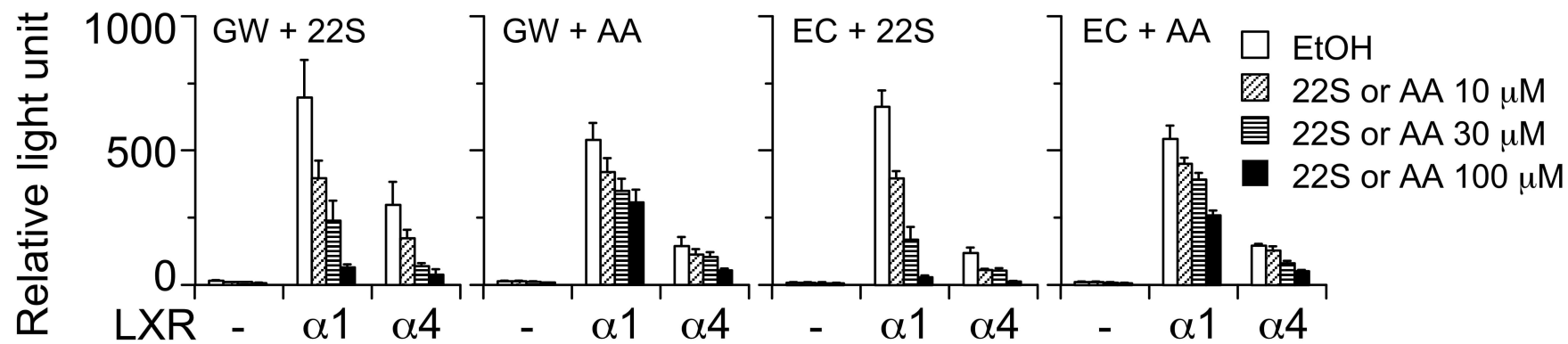
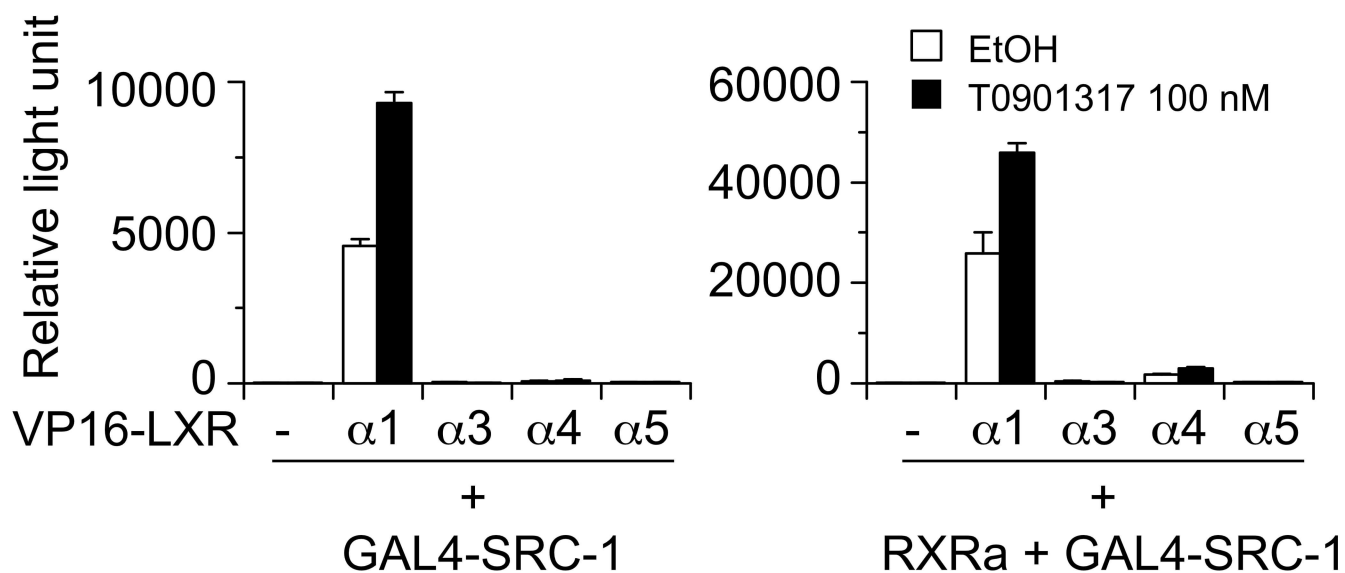
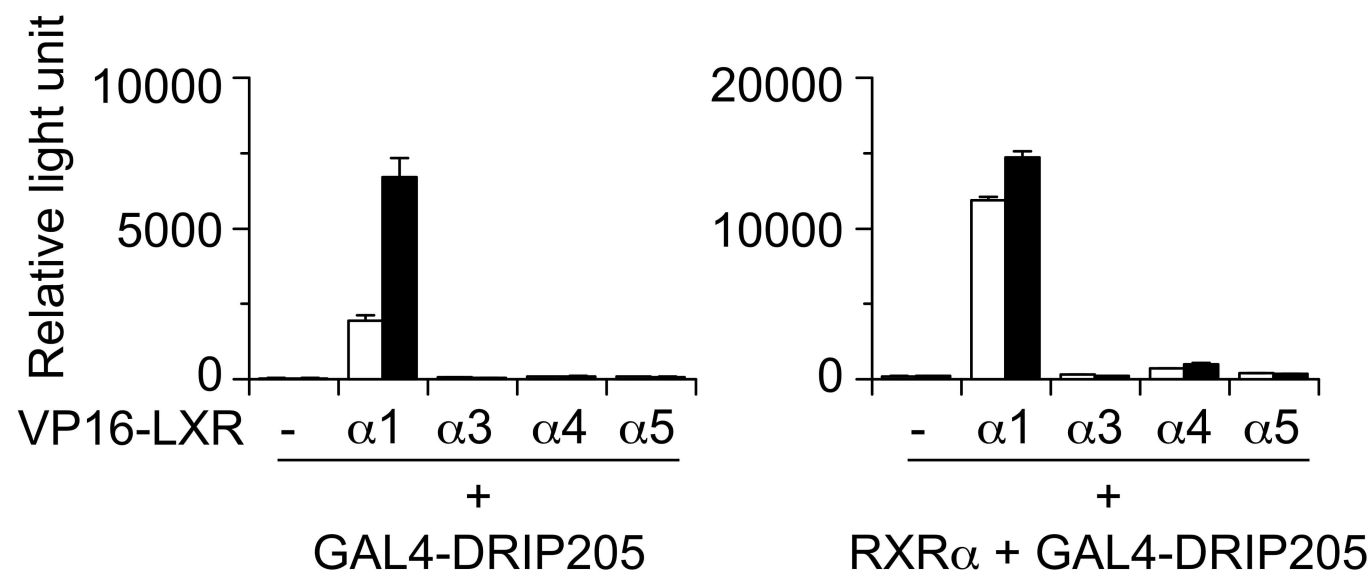


Fig. 8

A



B



C

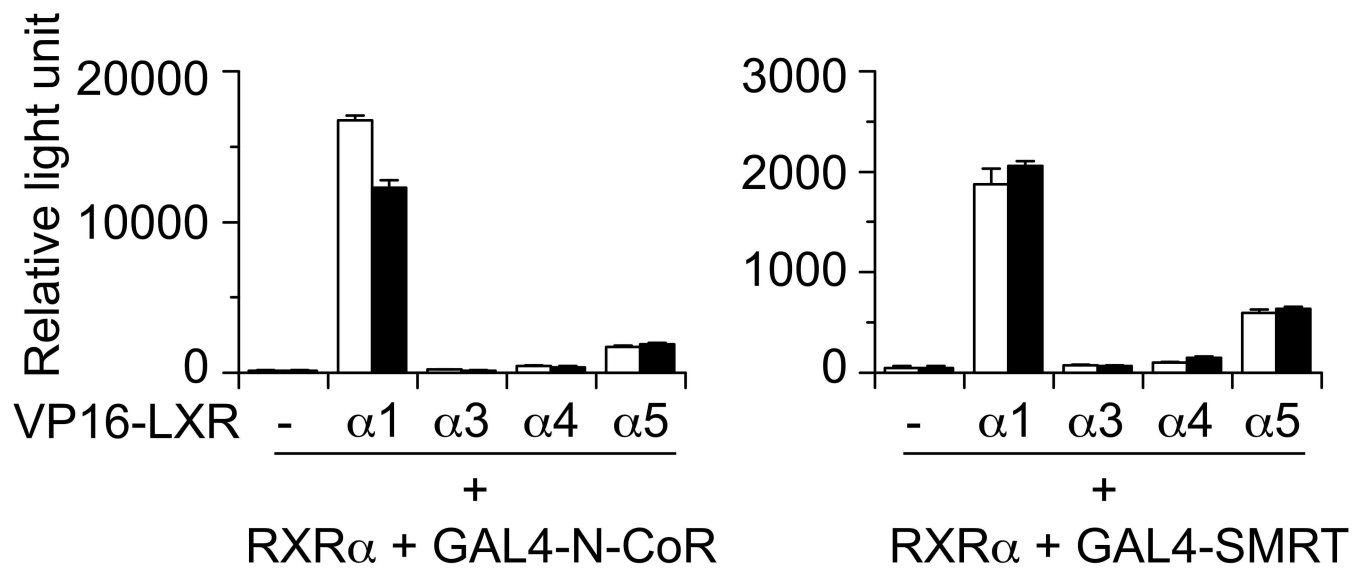
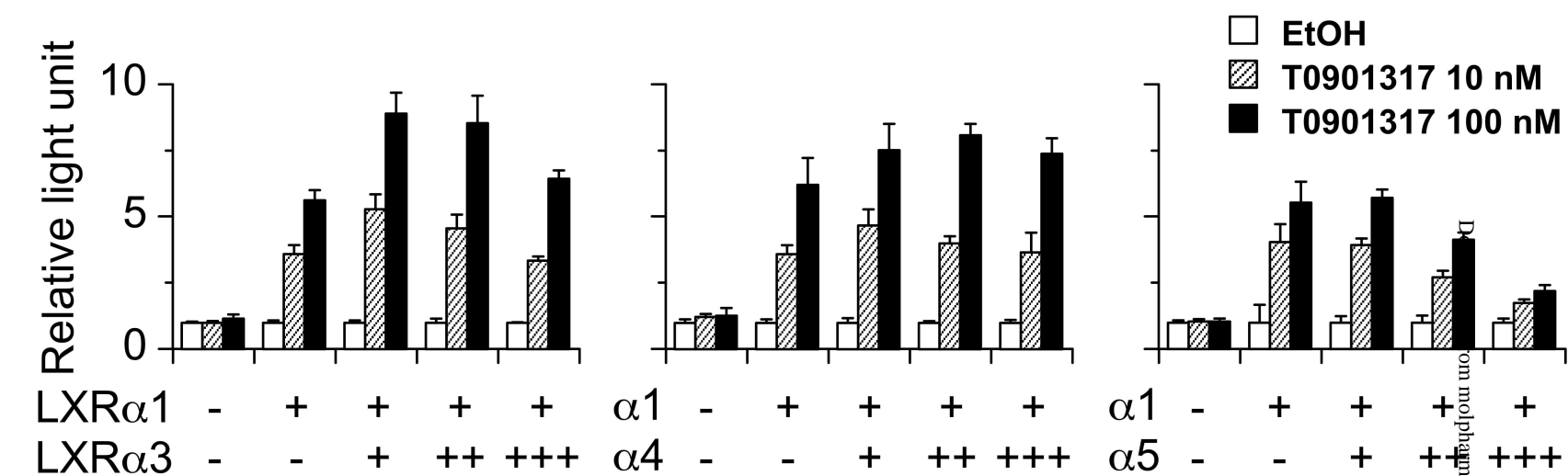
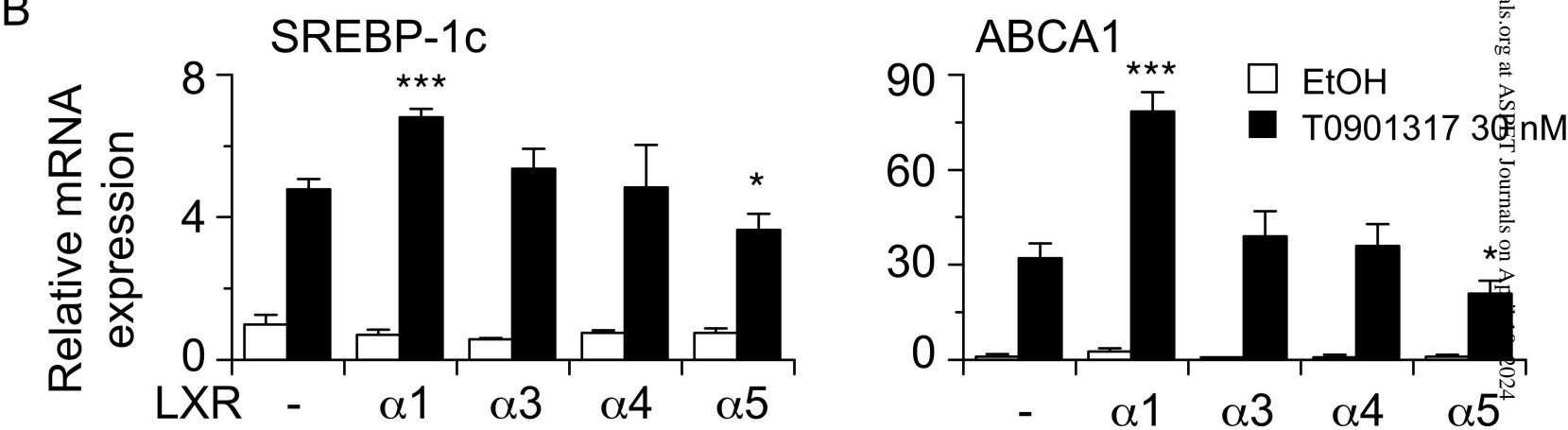


Fig.9

A



B



C

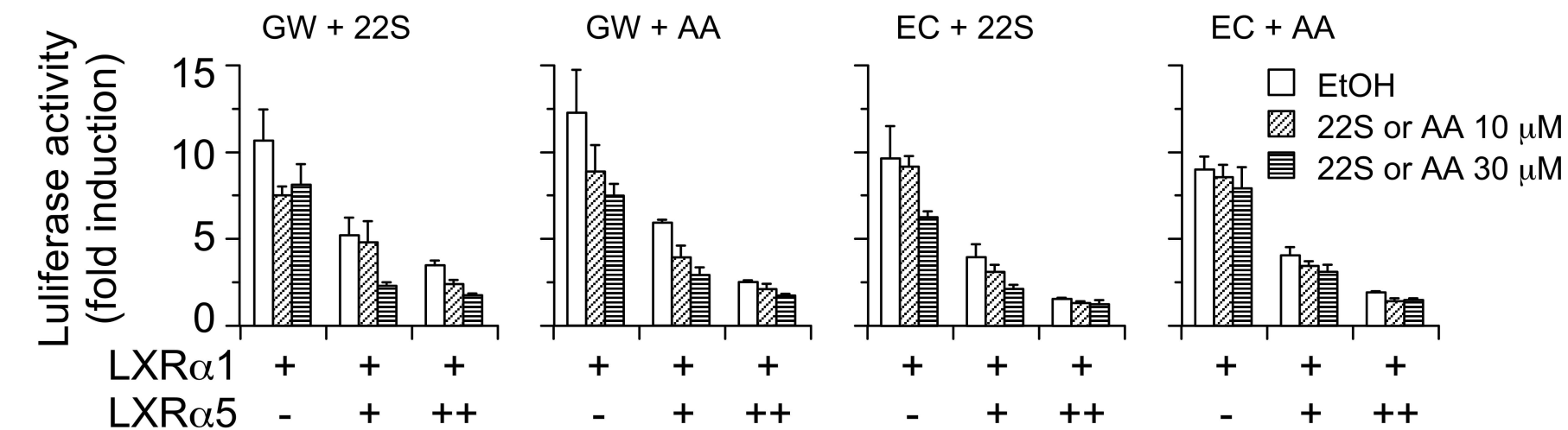


Fig. 10, A

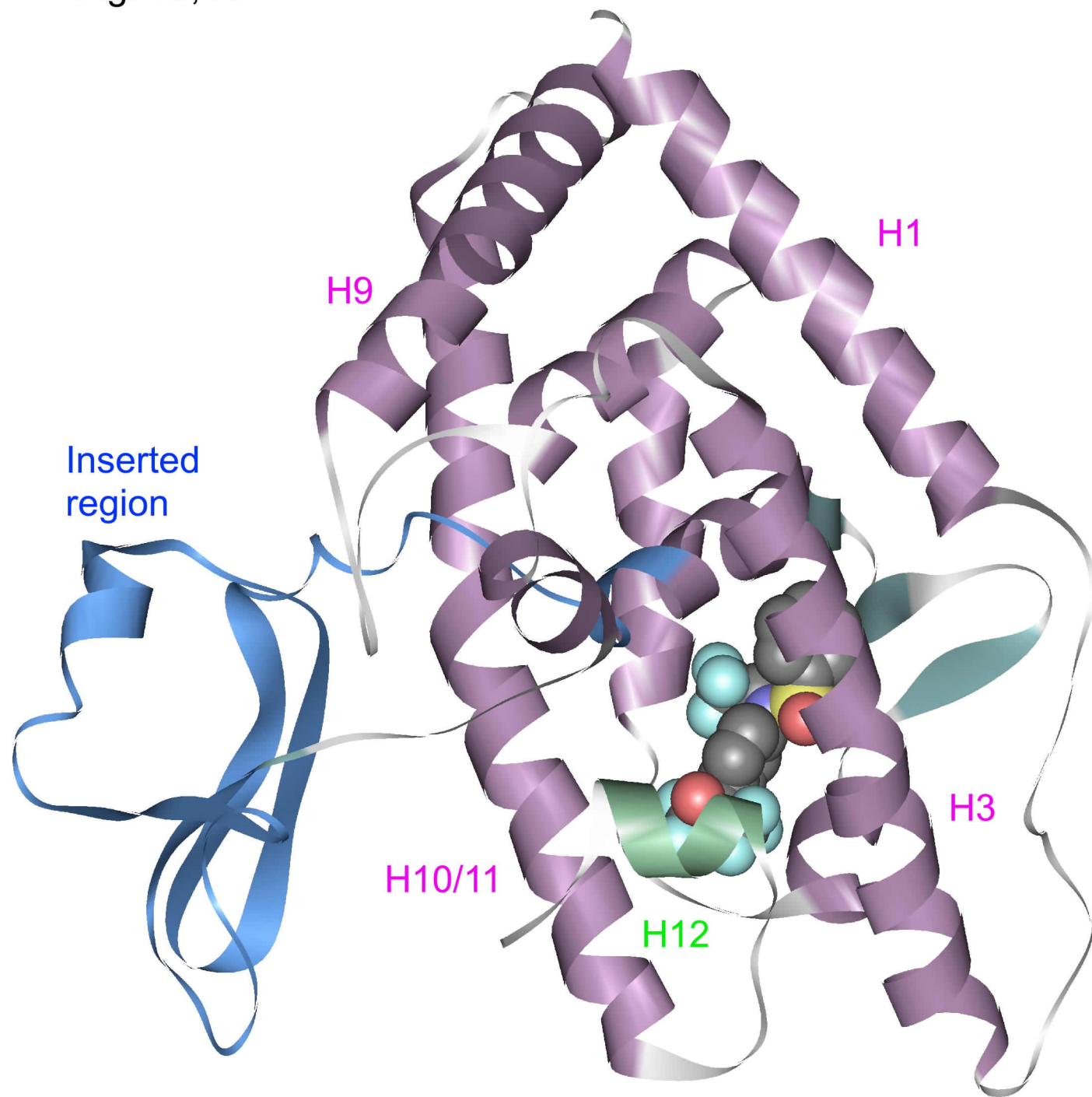


Fig. 10, B

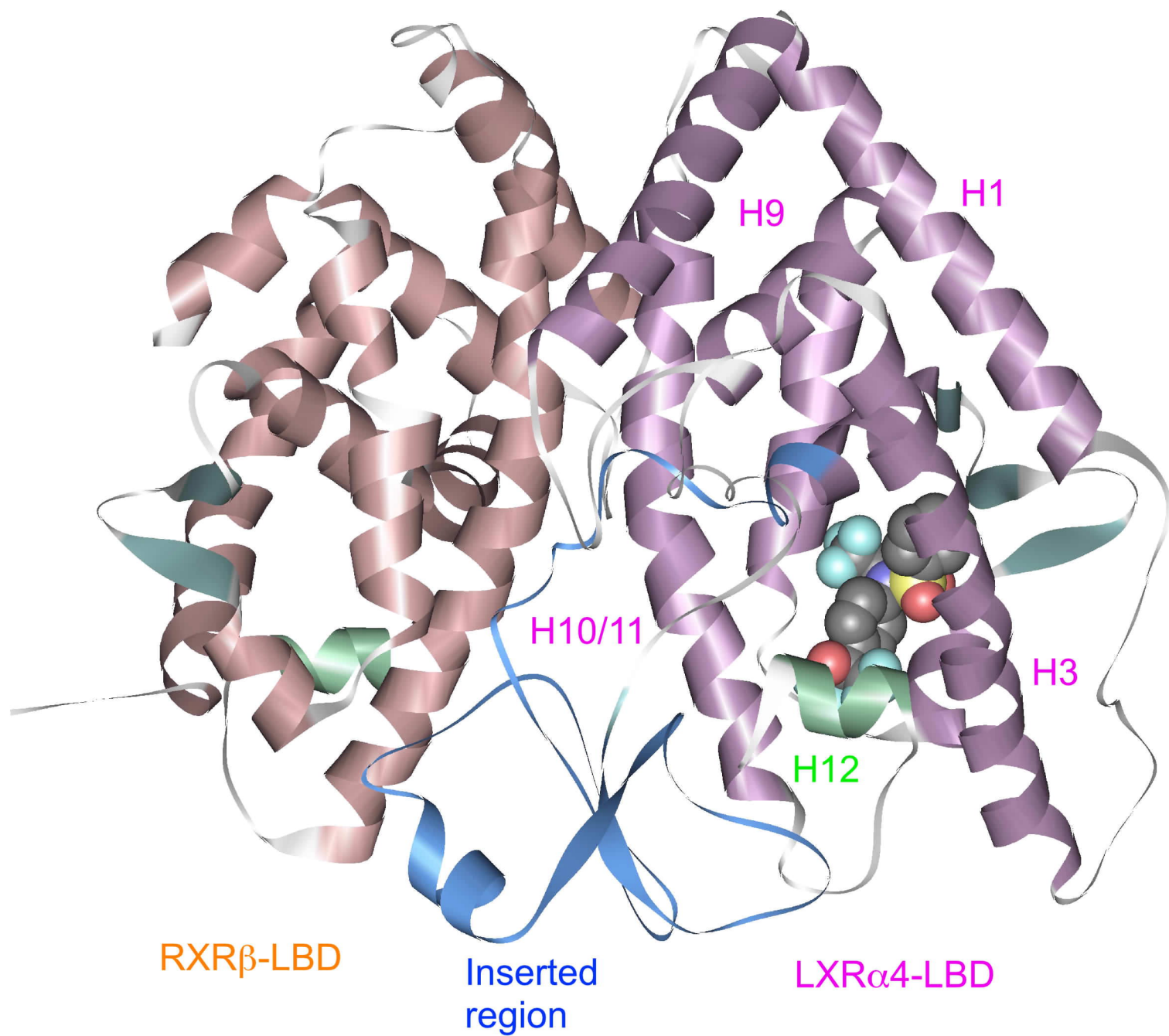


Fig. 10, C

